J. Fluid Mech. (1997), *vol.* 341, *pp.* 195–223. Printed in the United Kingdom

© 1997 Cambridge University Press

Two-dimensional long waves in turbulent flow over a sloping bottom

By ALLAN W. GWINN

Department of Atmospheric, Oceanic and Space Sciences, The University of Michigan, Ann Arbor, MI 48109-2143, USA
e-mail: gwinn@engin.umich.edu

(Received 1 August 1996 and in revised form 13 January 1997)

We investigate weakly two-dimensional weakly nonlinear weakly dispersive surface waves propagating in a turbulent flow over a gradually sloping bottom. The waves are shown to be governed by a turbulently damped variable-coefficient Kadomtsev–Petviashvili equation with periodic boundary conditions. Equations governing the lowest-order mean currents in both directions as well as the equation describing the lowest-order mean surface elevation are also derived. Solutions for the wave equation are found numerically using a Fourier pseudospectral technique in space and finite differencing in the time-like variable.

1. Introduction

Over the years, a considerable volume of theoretical research has been devoted to the study of long nonlinear water waves. It is clear that these waves are important features in a variety of environments. Standard water wave texts, such as Mei (1989), have extensive chapters devoted to explaining various details. In many investigations, the scope is restricted to ideal fluids; only a few have considered problems where viscous dissipation is important (see Mei 1989 for references). Although using ideal fluid models for long-wave phenomena is standard practice, the validity of ignoring dissipation is questionable (see for example Lighthill 1978, p. 464). Furthermore, if the dissipation is modelled solely by the inclusion of molecular viscosity, the results can be expected to be valid only in a laboratory setting since most natural oceanographic flows are turbulent. Clearly, turbulent bottom friction needs to be considered if one wishes to provide realistic dissipation mechanisms for shallow water flows.

Shuto (1976) proposed a turbulently damped Korteweg–deVries (KdV) equation to model one-dimensional flow over a gradually sloping bottom while Miles (1983) analysed the energy equation equivalent. Miles also referenced field observations that suggest the need to include turbulent bottom friction. Recently, Jacobs (1997) has resolved an inconsistency in the work of Shuto and Miles through a formal perturbation and matched asymptotic expansion analysis. Also, through numerical computation, Jacobs has verified Miles' prediction that a cnoidal wave propagating up a constant beach slope will develop into a train of solitary waves with a known amplitude to depth ratio.

Restricting their attention to constant depth but allowing weak two-dimensional effects, Segur & Finkel (1985) presented an analytical inviscid model based on doubly periodic solutions of the Kadomtsev–Petviashvili (KP) equation. For a recent review of many different physical phenomena modelled by various forms of inviscid KP

https://doi.org/10.1017/S0022112097005442 Published online by Cambridge University Press

equations, the reader is referred to Akylas (1994). Hammack, Scheffner & Segur (1989) conducted experiments to provide insight into the applicability of Segur & Finkel's model and a subsequent experiment (Hammack, Scheffner & Segur 1991) showed that weakly two-dimensional waves near a beach can generate periodic rip currents after breaking. Hammack *et al.* (1995) continued further along the lines of the 1989 investigation.

The next logical step to Segur & Finkel's inviscid two-dimensional study and Jacobs's one-dimensional turbulent investigation is a two-dimensional turbulent model. To this end, we incorporate variable topography and turbulent bottom friction into Segur & Finkel's model. The flow is found to consist of two asymptotic regions: an outer layer and a thin bottom boundary layer (the weaker top boundary layer is ignored). We are concerned primarily with calculating the flow outside the boundary layer; however, we analyse the boundary layer to provide expressions for the flow due to displacement thickness and to provide boundary conditions for the outer flow. We find that the surface elevation is governed by a turbulently damped KP equation whose coefficients depend on the water depth. Equations governing the mean surface and the horizontal currents are also derived. The numerical solution technique for the surface elevation is a Fourier pseudospectral method in space and a second-order finite difference scheme in the time-like variable.

We consider the case in which an initially known surface wave is allowed to propagate up a beach. Breaking effects are not modelled in this effort so our results are restricted to waves which do not break or to regions prior to breaking. Planar (genus 1) and non-planar (genus 2) solutions to the inviscid flat-bottomed KP equation as well as planar (straight-crested) and non-planar sinusoidal-like waves are used as initial conditions. Although the equations are derived for two-dimensional bottom topography, in the numerical experiments presented here we restrict the depth to be a function only of the cross-shore coordinate. In future efforts, we will explore various topographical configurations. The sinusoidal-like waves evolve into shapes very similar to their cnoidal counterparts as the depth decreases; however, the sinusoidal waves show stronger secondary peaks (planar case) or saddle regions (non-planar case). We also see the familiar hexagonal surface pattern of the non-planar waves described in previous investigations. The hexagons are seen at all depths but they gradually change shape. In addition, we find that non-planar waves generate periodic longshore currents at a lower order than planar waves. In all cases considered, the cross-shore bottom stress is positive (toward the shore) which produces a mean surface depression (setdown).

2. Formulation

To incorporate turbulent dissipation, the standard averaging process is employed leaving the Reynolds stresses to be modelled. We have chosen Donaldson's second-order turbulence model (Lewellen 1977) for this task; it has been shown to be useful for a wide variety of flows and is a relatively simple stress model. Consider three-dimensional turbulent flow in (x, y, z)-space with the fluid bounded above by a free surface $z = \zeta(x, y, t)$ and below by a rigid hydraulically rough surface $z = -d(x, y)$ (see figure 1). Let $\boldsymbol{u} = (u, v, w)$ denote the Reynolds-averaged velocity, p the Reynolds-averaged pressure, $\boldsymbol{\tau}$ the kinematic Reynolds stress tensor, $q^2/2$ the turbulent kinematic kinetic energy, and $q^3/(8\lambda)$ the rate of turbulent kinematic energy

https://doi.org/10.1017/S0022112097005442 Published online by Cambridge University Press

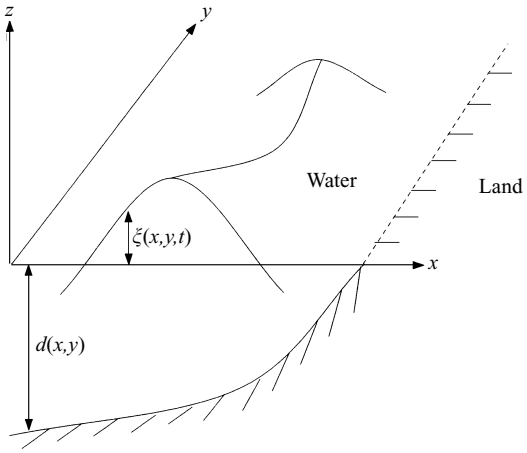


FIGURE 1. Schematic diagram of the coordinate system.

dissipation. The governing equations for Donaldson's turbulence model are

$$\nabla \cdot \boldsymbol{u} = 0, \tag{2.1}$$

$$\frac{\mathrm{D}\boldsymbol{u}}{\mathrm{D}t} + \frac{1}{\rho}\nabla p = \nabla \cdot \boldsymbol{\tau} - g\hat{\boldsymbol{k}}, \tag{2.2}$$

$$\frac{\mathrm{D}\boldsymbol{\tau}}{\mathrm{D}t} + \boldsymbol{\tau} \cdot \nabla \boldsymbol{u} + (\boldsymbol{\tau} \cdot \nabla \boldsymbol{u})^{\dagger} = c_1 \nabla \cdot (q\lambda \nabla \boldsymbol{\tau}) - \frac{q}{\lambda}\left(\boldsymbol{\tau} + \frac{q^2}{4}\boldsymbol{I}\right), \tag{2.3}$$

$$\frac{\mathrm{D}q^2}{\mathrm{D}t} = 2\boldsymbol{\tau} : \nabla \boldsymbol{u} + c_1 \nabla \cdot \left(q\lambda \nabla q^2\right) - \frac{q^3}{4\lambda}, \tag{2.4}$$

$$\frac{\mathrm{D}\lambda}{\mathrm{D}t} = c_1 \nabla \cdot (q\lambda \nabla \lambda) + c_2 q - c_3 \frac{\lambda}{q^2}\boldsymbol{\tau} : \nabla \boldsymbol{u} - \frac{c_4}{q}\left|\nabla (q\lambda)\right|^2, \tag{2.5}$$

where $\mathrm{D}/\mathrm{D}t = \partial/\partial t + \boldsymbol{u} \cdot \nabla$, g is the gravitational constant, ρ is the density of water, $\hat{\boldsymbol{i}}$, $\hat{\boldsymbol{j}}$, and $\hat{\boldsymbol{k}}$ are unit vectors along the coordinate axes, $\boldsymbol{I}$ is the identity tensor, the superscript † denotes the transpose, : is the tensor inner product (i.e. for Cartesian tensors $\boldsymbol{a}$ and $\boldsymbol{b}$, $\boldsymbol{a}:\boldsymbol{b} = \sum_i \sum_j a_{ij} b_{ji}$), and molecular viscosity is ignored. The constants in the above equations and an additional constant c_5 are given by

$$c_1 = 0.3, \quad c_2 = 0.04375 + \left(0.15\sqrt{2}\right)\kappa^2, \tag{2.6}$$

$$c_3 = 0.35, \quad c_4 = 0.375, \quad c_5 = 2^{3/4}\kappa, \tag{2.7}$$

in which $\kappa = 0.4$ is the Kármán constant.

We define $(\hat{\boldsymbol{S}}_1, \hat{\boldsymbol{S}}_2, \hat{\boldsymbol{N}})$ as surface-fitting curvilinear unit vectors which reduce to $(\hat{\boldsymbol{i}}, \hat{\boldsymbol{j}}, \hat{\boldsymbol{k}})$ when there are no waves (see Appendix A). The kinematic and dynamic boundary conditions at $z = \zeta$ are

$$w = \frac{\partial \zeta}{\partial t} + u\frac{\partial \zeta}{\partial x} + v\frac{\partial \zeta}{\partial y}, \quad \tau_{NS_1} = 0, \quad \tau_{NS_2} = 0, \quad p = \rho \tau_{NN}. \tag{2.8}$$

Standard practice involving turbulent flow under a free surface treats that surface as

https://doi.org/10.1017/S0022112097005442 Published online by Cambridge University Press

a symmetry plane; therefore, we also impose

$$\hat{\boldsymbol{N}} \cdot \nabla \left(\tau_{S_1S_1}, \tau_{S_1S_2}, \tau_{S_2S_2}, \tau_{NN}, q, \lambda\right) = 0, \tag{2.9}$$

at $z = \zeta$.

At the bottom surface, we define $(\hat{\boldsymbol{s}}_1, \hat{\boldsymbol{s}}_2, \hat{\boldsymbol{n}})$ as surface-fitting curvilinear unit vectors which reduce to $(\hat{\boldsymbol{i}}, \hat{\boldsymbol{j}}, \hat{\boldsymbol{k}})$ for a flat bottom (see Appendix A). We also define z_0 as the bottom roughness length, n as the distance into the fluid measured along $\hat{\boldsymbol{n}}$, and $\boldsymbol{\sigma}$ as the bottom friction velocity (defined to be tangent to the surface). With these definitions, the boundary conditions are

$$\boldsymbol{u} - \hat{\boldsymbol{n}}\left(\hat{\boldsymbol{n}} \cdot \boldsymbol{u}\right) \rightarrow \frac{\boldsymbol{\sigma}}{\kappa} \ln\left(\frac{n}{z_0}\right), \quad \boldsymbol{u} \cdot \hat{\boldsymbol{n}} \rightarrow 0, \tag{2.10}$$

$$\boldsymbol{\tau} \rightarrow |\boldsymbol{\sigma}|\left(\hat{\boldsymbol{n}}\boldsymbol{\sigma} + \boldsymbol{\sigma}\hat{\boldsymbol{n}}\right) - 2^{1/2}\left(|\boldsymbol{\sigma}|^2 \boldsymbol{I} + \boldsymbol{\sigma}\boldsymbol{\sigma}\right), \tag{2.11}$$

$$q \rightarrow 2^{5/4}|\boldsymbol{\sigma}|, \quad \lambda \rightarrow c_5 n, \tag{2.12}$$

as $z \rightarrow -d$.

We want to incorporate the effects of weak nonlinearity, weak dispersion, weak dissipation, and weak two-dimensionality. To do this in a formal way, we will first non-dimensionalize the equations, after which we will define several small non-dimensional parameters. Relationships between these small parameters will be assumed in order to examine the general case in which all the above effects enter in the force balance at the same order; this will also allow us to perform a perturbation expansion in one of the small parameters.

We define (k_0, l_0) as a characteristic wavenumber vector, d_0 as a characteristic depth, L_0 as a characteristic scale on which d varies in the x-direction, $c_0 = (gd_0)^{1/2}$ as a characteristic phase speed in the x-direction, Γ_0 as a characteristic particle velocity in the x-direction, $\omega_0 = c_0 k_0$ as a characteristic frequency, and u_τ as a characteristic friction velocity in the x-direction. Denoting non-dimensional values by asterisks, we scale the equations using these characteristic values as follows:

$$\left(x^*, y^*, z^*\right) = \left(xk_0, yl_0, \frac{z}{d_0}\right), \quad (u, v, w) = \left(u^*, v^*\frac{l_0}{k_0}, w^* k_0 d_0\right)\Gamma_0, \tag{2.13}$$

$$t^* = t\omega_0, \quad p^* = \frac{p + \rho g z}{\rho c_0 \Gamma_0}, \quad \zeta^* = \frac{c_0 \zeta}{d_0 \Gamma_0}, \quad d^* = \frac{d}{d_0}, \tag{2.14}$$

$$\left(\tau_{xz}, \tau_{xx}, \tau_{yy}, \tau_{zz}\right) = \left(\tau^*_{xz}, \tau^*_{xx}, \tau^*_{yy}, \tau^*_{zz}\right) u_\tau^2,$$

$$\left(\tau_{yz}, \tau_{xy}\right) = \left(\tau^*_{yz}, \tau^*_{xy}\right) u_\tau^2 \frac{l_0}{k_0}, \tag{2.15}$$

$$q = q^* u_\tau, \quad \lambda = \lambda^* d_0, \quad \left(\sigma_x, \sigma_y\right) = \left(\sigma^*_x, \sigma^*_y \frac{l_0}{k_0}\right) u_\tau. \tag{2.16}$$

Here we are assuming that the dominant propagation direction of the waves is in the x-direction. Henceforth, we will omit asterisks and remind the reader that variables are all dimensionless unless stated otherwise.

After scaling, it is convenient to define the following non-dimensional parameters:

$$\alpha = \frac{\Gamma_0}{c_0}, \quad \epsilon = \frac{u_\tau}{\Gamma_0}, \quad \left(\delta_x, \delta_y\right) = (k_0, l_0)\, d_0, \quad \left(\gamma_x, \gamma_y\right) = \frac{\left(k_0^{-1}, l_0^{-1}\right)}{L_0}. \tag{2.17}$$

https://doi.org/10.1017/S0022112097005442 Published online by Cambridge University Press

Physically, α is a measure of nonlinearity, ϵ is the square root of a characteristic drag coefficient, δ_x and δ_y measure dispersion in the x- and y-directions respectively, and γ_x and γ_y are the ratios of the x and y length scales of the waves to the depth variation. Thus, the dimensionless depth d is a function of $(\gamma_x x, \gamma_y y)$. We follow Johnson (1983) in requiring nonlinearity, x-dispersion, x-directed bottom slope, and two-dimensional effects to be in balance. Since the turbulent body force in the horizontal momentum equations is $O(\alpha\epsilon^2/\delta_x)$, turbulence and the other effects are in balance when

$$\alpha = A\epsilon^4, \quad \delta_x = B\epsilon^2, \quad \delta_y = C\epsilon^4, \quad \gamma_x = D\epsilon^4, \quad \gamma_y = E\epsilon^6, \tag{2.18}$$

where A, B, C, D, E are all $O(1)$ constants. These parameters may subsequently be taken large or small if one of these effects is deemed to be relatively unimportant.

We will consider flows in which $\epsilon \ll 1$. The dimensionless equations with $O(\epsilon^6)$ errors in the continuity and momentum equations, and $O(\epsilon^4)$ errors in the turbulence equations, are

$$\frac{\partial u}{\partial x} + \epsilon^4 \left(\frac{C}{B}\right)^2 \frac{\partial v}{\partial y} + \frac{\partial w}{\partial z} = 0, \tag{2.19}$$

$$\frac{\mathrm{D}u}{\mathrm{D}t} + \frac{\partial p}{\partial x} = \frac{A}{B}\epsilon^4 \frac{\partial \tau_{zx}}{\partial z}, \tag{2.20}$$

$$\frac{\mathrm{D}v}{\mathrm{D}t} + \frac{\partial p}{\partial y} = \frac{A}{B}\epsilon^4 \frac{\partial \tau_{zy}}{\partial z}, \tag{2.21}$$

$$B^2\epsilon^4 \frac{\partial w}{\partial t} + \frac{\partial p}{\partial z} = 0, \tag{2.22}$$

$$\frac{\mathrm{D}\tau_{zx}}{\mathrm{D}t} + \frac{A}{B}\epsilon^2 \tau_{zz} \frac{\partial u}{\partial z} = \frac{A}{B}\epsilon^3 \left[c_1 \frac{\partial}{\partial z}\left(q\lambda \frac{\partial \tau_{zx}}{\partial z}\right) - \frac{q}{\lambda}\tau_{zx}\right], \tag{2.23}$$

$$\frac{\mathrm{D}\tau_{zy}}{\mathrm{D}t} + \frac{A}{B}\epsilon^2 \tau_{zz} \frac{\partial v}{\partial z} = \frac{A}{B}\epsilon^3 \left[c_1 \frac{\partial}{\partial z}\left(q\lambda \frac{\partial \tau_{zy}}{\partial z}\right) - \frac{q}{\lambda}\tau_{zy}\right], \tag{2.24}$$

$$\frac{\mathrm{D}\tau_{zz}}{\mathrm{D}t} + 2A\epsilon^4 \tau_{zz} \frac{\partial w}{\partial z} = \frac{A}{B}\epsilon^3 \left[c_1 \frac{\partial}{\partial z}\left(q\lambda \frac{\partial \tau_{zz}}{\partial z}\right) - \frac{q}{\lambda}\left(\tau_{zz} + \frac{q^3}{4}\right)\right], \tag{2.25}$$

$$\frac{\mathrm{D}q^2}{\mathrm{D}t} - 2\frac{A}{B}\epsilon^2 \tau_{zx} \frac{\partial u}{\partial z} = \frac{A}{B}\epsilon^3 \left[c_1 \frac{\partial}{\partial z}\left(q\lambda \frac{\partial q^2}{\partial z}\right) - \frac{q^3}{4\lambda}\right], \tag{2.26}$$

$$\frac{\mathrm{D}\lambda}{\mathrm{D}t} + \frac{A}{B}\epsilon^2 \frac{c_3\lambda}{q^2}\tau_{zx} \frac{\partial u}{\partial z} = \frac{A}{B}\epsilon^3 \left[c_1 \frac{\partial}{\partial z}\left(q\lambda \frac{\partial \lambda}{\partial z}\right) + c_2 q - \frac{c_4}{q}\left(\frac{\partial q\lambda}{\partial z}\right)^2\right], \tag{2.27}$$

where

$$\frac{\mathrm{D}}{\mathrm{D}t} = \frac{\partial}{\partial t} + A\epsilon^4 \left(u\frac{\partial}{\partial x} + w\frac{\partial}{\partial z}\right). \tag{2.28}$$

With $O(\epsilon^6)$ or higher errors on the velocity and pressure and with $O(\epsilon^4)$ errors on the turbulence quantities, the top boundary conditions are

$$w = \frac{\partial \zeta}{\partial t} + A\epsilon^4 \frac{\partial u\zeta}{\partial x}, \quad p = \zeta, \quad \tau_{zx} = \tau_{zy} = \frac{\partial}{\partial z}(\tau_{zz}, q, \lambda) = 0, \tag{2.29}$$

at $z = 0$. The bottom boundary conditions are

$$u \to \sigma_x \left[\Upsilon + \frac{\epsilon}{\kappa} \ln \frac{B(z+d)}{A\epsilon^3}\right], \quad v \to \sigma_y \left[\Upsilon + \frac{\epsilon}{\kappa} \ln \frac{B(z+d)}{A\epsilon^3}\right], \tag{2.30}$$

https://doi.org/10.1017/S0022112097005442 Published online by Cambridge University Press

$$w \to -A\epsilon^4 umD, \quad q \to 2^{5/4}\,|\boldsymbol{\sigma}|\,, \quad \lambda \to c_5\,(z+d)\,, \tag{2.31}$$

$$\tau_{zx} \to |\boldsymbol{\sigma}|\,\sigma_x, \quad \tau_{zy} \to |\boldsymbol{\sigma}|\,\sigma_y, \quad \tau_{zz} \to -2^{1/2}\,|\boldsymbol{\sigma}|^2\,, \tag{2.32}$$

as $z \to -d$, where

$$\Upsilon = \frac{\epsilon}{\kappa}\ln\frac{\epsilon\Gamma_0}{\omega_0 z_0}, \quad m = \frac{1}{\gamma_x}\frac{\partial}{\partial x}d\left(\gamma_x x, \gamma_y y\right) \tag{2.33}$$

are $O\,(1)$ quantities (see Jacobs 1990 for an extensive discussion of Υ) and where

$$\boldsymbol{\sigma} = \hat{\boldsymbol{i}}\sigma_x + \hat{\boldsymbol{j}}\frac{C}{B}\epsilon^2\sigma_y. \tag{2.34}$$

As boundary conditions at $x = 0$, we require that

$$\underline{\zeta} = 0, \quad \underline{\boldsymbol{u}} = O\left(\epsilon^4\right), \tag{2.35}$$

where the underbar denotes averages over the phase. (The phase variable is defined in equation (3.1) below.) The first condition defines the offshore mean depth to be d. The other condition is equivalent to the offshore mean velocity having a magnitude on the order of the Stokes drift.

The field equations show a small parameter multiplying the most highly differentiated terms, implying the presence of a boundary layer. Consequently, we will treat this system of equations by the method of matched asymptotic expansions (Van Dyke 1975). We first analyse the flow outside the boundary layer to derive an equation governing the waves and equations governing the mean currents and mean surface level. These equations include effects due to turbulence stresses and the flow due to displacement thickness for which explicit expressions are found by examining the boundary layer.

3. Outer flow

To treat the outer layer, we follow Johnson (1983) and introduce the following multiple scale variables:

$$r = \frac{1}{\alpha}\Theta\,(X, Y\,) - t, \quad X = \alpha x, \quad Y = \alpha y, \tag{3.1}$$

where, to make a slight generalization of Johnson, we have defined

$$\Theta = \theta + \alpha\phi + \ldots. \tag{3.2}$$

These coordinates anticipate changes in the phase speed due to the inhomogeneity of the propagation medium. Moreover, following Segur & Finkel (1985), we require periodicity in the r- and y-coordinates; however, because we have variable topography (in terms of the slow variables, we have $d = d(D/A)X, (EB\delta_y/AC\delta_x)Y\,)$ the flow is not, in general, periodic in X and Y. Using the chain rule, the differentiation operators transform as follows:

$$\left.\begin{aligned} \frac{\partial}{\partial t} &= -\frac{\partial}{\partial r}, \quad \frac{\partial}{\partial x} = \frac{\partial\theta}{\partial X}\frac{\partial}{\partial r} + \alpha\left(\frac{\partial}{\partial X} + \frac{\partial\phi}{\partial X}\frac{\partial}{\partial r}\right), \\ \frac{\partial}{\partial y} &= \frac{\partial}{\partial y} + \frac{\partial\theta}{\partial Y}\frac{\partial}{\partial r} + \alpha\left(\frac{\partial}{\partial Y} + \frac{\partial\phi}{\partial Y}\frac{\partial}{\partial r}\right). \end{aligned}\right\} \tag{3.3}$$

We will expand the dependent variables in the form

$$f = f_0 + \epsilon f_1 + \epsilon^2 f_2 + \ldots, \quad \tau_{\cdot\cdot} = \tau_{\cdot\cdot}^{(0)} + \epsilon\tau_{\cdot\cdot}^{(1)} + \epsilon^2\tau_{\cdot\cdot}^{(2)} + \ldots, \tag{3.4}$$

https://doi.org/10.1017/S0022112097005442 Published online by Cambridge University Press

where $\tau_{\cdot\cdot}$ denotes an arbitrary stress component. We will also assume here and verify later that the vertical velocity outside of the boundary layer satisfies

$$w \to \epsilon^4 \left(\Omega - Au \frac{\partial d}{\partial X} \right), \tag{3.5}$$

as $z \to -d$ with $O\left(\epsilon^6\right)$ errors, where $\epsilon^4 \Omega$ is the flow due to displacement thickness. Our aim is to derive equations for the dominant contributions to the surface elevation and the horizontal velocity.

Substituting (3.3) and (3.4) into the equations in §2 and equating like powers of ϵ yields

$$\left.\begin{aligned} p_k = h_k + H_k = \zeta_k, \quad u_k = \frac{\partial \theta}{\partial X} h_k + U_k, \\ w_k = -\left(\frac{\partial \theta}{\partial X} \right)^2 \frac{\partial h_k}{\partial r} (z+d), \quad \frac{\partial v_k}{\partial r} = \frac{\partial \theta}{\partial Y} \frac{\partial h_k}{\partial r} + \frac{\partial}{\partial y} (h_k + H_k), \end{aligned}\right\} \tag{3.6}$$

for $k = 0, 1, 2, 3$, where h_k is a zero-mean periodic function of r. H_k and U_k are not functions of r; H_k is the r-averaged surface elevation (setdown if H is negative) and U_k is the mean velocity in the x-direction. Using the top boundary condition on w_k provides a relation governing the lowest-order non-dimensional phase speed $\left(C_p^{(0)}\right)$:

$$\left(\frac{\partial \theta}{\partial X} \right)^2 = d^{-1} \equiv \frac{1}{\left[C_p^{(0)} \right]^2}. \tag{3.7}$$

In order to prevent a secularity in the solution for v_k, we must have

$$\frac{\partial H_k}{\partial y} = 0. \tag{3.8}$$

For subsequent convenience, we will also denote

$$v_k = \tilde{v_k}(r, y, X, Y) + V_k(y, X, Y, z), \quad \underline{\tilde{v_k}} = 0. \tag{3.9}$$

We remind the reader that the underbar denotes averaging over r.

From the turbulence equations, we obtain

$$\frac{\partial}{\partial r} \left(\tau_{zx}^{(j)}, \tau_{zy}^{(j)}, q_j, \lambda_j \right) = 0, \quad \frac{\partial}{\partial r} \tau_{zz}^{(l)} = 0, \tag{3.10}$$

for $j = 0, 1$ and $l = 0, 1, 2$. At $O\left(\epsilon^2\right)$, equations (2.23) and (2.24) become

$$\frac{\partial}{\partial r} \left(\tau_{zx}^{(2)}, \tau_{zy}^{(2)} \right) = \frac{A}{B} \tau_{zz}^{(0)} \left(\frac{\partial U_0}{\partial z}, \frac{\partial V_0}{\partial z} \right). \tag{3.11}$$

In order to avoid a secularity in the solution for $\tau_{zx}^{(2)}$ and $\tau_{zx}^{(2)}$, we must have

$$\frac{\partial U_0}{\partial z} = \frac{\partial V_0}{\partial z} = 0, \tag{3.12}$$

and thus the lowest-order r-averaged horizontal velocity components are independent of z.

At $O\left(\epsilon^3\right)$, the equation for τ_{zx} is of the form

$$-\frac{\partial \tau_{zx}^{(3)}}{\partial r} + \frac{A}{B} \tau_{zz}^{(0)} \frac{\partial U_1}{\partial z} = \frac{A}{B} \mathscr{G}, \tag{3.13}$$

https://doi.org/10.1017/S0022112097005442 Published online by Cambridge University Press

where $\mathscr{G}$ involves other zeroth-order variables and is independent of r; similar forms are found for the other turbulence quantities. To avoid secularities, the compatibility conditions for the turbulence quantities are

$$\tau_{zz}^{(0)}\frac{\partial U_1}{\partial z} = c_1\frac{\partial}{\partial z}\left(q_0\lambda_0\frac{\partial \tau_{zx}^{(0)}}{\partial z}\right) - \frac{q_0}{\lambda_0}\tau_{xz}^{(0)}, \tag{3.14}$$

$$c_1\frac{\partial}{\partial z}\left(q_0\lambda_0\frac{\partial \tau_{zz}^{(0)}}{\partial z}\right) = \frac{q_0}{\lambda_0}\left(\tau_{zz}^{(0)} + \frac{q_0^2}{4}\right), \tag{3.15}$$

$$2\tau_{zx}^{(0)}\frac{\partial U_1}{\partial z} + c_1\frac{\partial}{\partial z}\left(q_0\lambda_0\frac{\partial q_0^2}{\partial z}\right) = \frac{q_0^3}{4\lambda_0}, \tag{3.16}$$

$$\frac{c_3\lambda_0}{q_0^2}\tau_{zx}^{(0)}\frac{\partial U_1}{\partial z} = c_1\frac{\partial}{\partial z}\left(q_0\lambda_0\frac{\partial \lambda_0}{\partial z}\right) + c_2q_0 - \frac{c_4}{q_0}\left[\frac{\partial}{\partial z}(q_0\lambda_0)\right]^2. \tag{3.17}$$

Equations (3.14)–(3.17) are the field equations governing the $O(\epsilon)$ mean cross-shore velocity and the zeroth-order stresses.

At $O(\epsilon^4)$, it is easily found that

$$\zeta_4 = H_4 + h_4, \quad p_4 = -B^2\left(z + \frac{1}{2}\frac{z^2}{d}\right)H_4 + h_4. \tag{3.18}$$

The continuity and x-momentum equations at this order are

$$\frac{\partial\theta}{\partial X}\frac{\partial u_4}{\partial r} + \frac{\partial w_4}{\partial z} + A\left(\frac{\partial u_0}{\partial X} + \frac{\partial\phi}{\partial X}\frac{\partial u_0}{\partial r}\right) + \left(\frac{C}{B}\right)^2\left(\frac{\partial v_0}{\partial y} + \frac{\partial\theta}{\partial Y}\frac{\partial v_0}{\partial r}\right) = 0, \tag{3.19}$$

$$-\frac{\partial u_4}{\partial r} + \frac{\partial p_4}{\partial r}\frac{\partial\theta}{\partial X} + A\left(u_0\frac{\partial u_0}{\partial r}\frac{\partial\theta}{\partial X} + \frac{\partial p_0}{\partial X} + \frac{\partial\phi}{\partial X}\frac{\partial p_0}{\partial r}\right) = \frac{A}{B}\frac{\partial\tau_{zx}^{(0)}}{\partial z}, \tag{3.20}$$

and the boundary conditions on w_4 are

$$w_4 = -\frac{\partial\zeta_4}{\partial r} + A\frac{\partial\theta}{\partial X}\frac{\partial u_0\zeta_0}{\partial r}, \quad w_4 = \Omega_0 - Au_0\frac{\partial d}{\partial X}, \tag{3.21}$$

at $z = 0$ and $z = -d$ respectively. If we average the x-momentum equation (3.20) over r, we obtain

$$B\frac{\partial H_0}{\partial X} = \frac{\partial\tau_{zx}^{(0)}}{\partial z}, \tag{3.22}$$

which after integrating and using the top boundary condition on the shear stress (2.29) gives

$$\tau_{zx}^{(0)} = zB\frac{\partial H_0}{\partial X}. \tag{3.23}$$

Once the boundary condition on $\tau_{zx}^{(0)}$ at the bottom of the outer layer is found, (3.23) applied at $z = -d$ provides an equation governing the mean surface level. Because of (3.8), (3.23) implies that $\tau_{zx}^{(0)}$ is independent of y. Since, the $O(\epsilon)$ r-averaged cross-shore velocity is driven by the zeroth-order bottom stress, it too will be independent of y. Thus, to obtain y-variability in the cross-shore current, one must go to a higher order; this task will be examined in a later effort.

Eliminating u_4 between the continuity and x-momentum equations, using (3.21) and (3.22), and integrating over z from $-d$ to 0, produces an equation for h_0. Examining

https://doi.org/10.1017/S0022112097005442 Published online by Cambridge University Press

travelling waves whose main propagation direction is in the $+x$ direction such that

$$\frac{\partial\theta}{\partial X} = d^{-1/2}, \quad \theta = \int_0^X d^{-1/2}\,\mathrm{d}X \tag{3.24}$$

and letting

$$\frac{\partial\phi}{\partial X} = -\frac{1}{d}\left(U_0 + \frac{H_0}{2d^{1/2}}\right), \tag{3.25}$$

for the Doppler correction (where ϕ is defined in equation (3.2)), the equation for h_0 becomes

$$2d^{1/2}\frac{\partial h_0}{\partial X} + 3d^{-1}h_0\frac{\partial h_0}{\partial r} + \frac{d}{3}\frac{B^2}{A}\frac{\partial^3 h_0}{\partial r^3} + \frac{\partial}{\partial X}(U_0 d) + \frac{1}{2d^{1/2}}h_0\frac{\partial d}{\partial X} + \frac{d}{A}\left(\frac{C}{B}\right)^2\left[\frac{\partial v_0}{\partial y} + \frac{\partial\theta}{\partial Y}\left(\frac{\partial h_0}{\partial y} + \frac{\partial h_0}{\partial r}\frac{\partial\theta}{\partial Y}\right)\right] = \frac{\Omega_0}{A}. \tag{3.26}$$

In (3.25), we have assumed that U_0 is only a function of the slow variables X and Y in concert with the above discussion regarding the lack of y-variability in H_0, $\tau_{zx}^{(0)}$, and U_1. In fact, since we have intitially assumed only the presence of an offshore zero-mean periodic wave and no ambient currents (see (2.35)), U_0 should be zero because all averaged velocities must be smaller than the characteristic orbital velocity Γ_0. (The only mechanisms which can generate currents in this work have been required to be small.) This will be shown in §5, and we will carry along U_0 in our calculations until then.

If we average (3.26) over r, we obtain

$$\frac{\partial}{\partial X}(U_0 d) + \frac{d}{A}\left(\frac{C}{B}\right)^2\frac{\partial V_0}{\partial y} = \frac{1}{A}\underline{\Omega}_0, \tag{3.27}$$

and if we average (3.27) over y (denoted by angle brackets) while insisting on y-periodicity, we have

$$\frac{\partial}{\partial X}(U_0 d) = \frac{1}{A}\langle\underline{\Omega}_0\rangle. \tag{3.28}$$

After examination of the boundary layer, Ω_0 can be found and (3.28) will provide an equation to determine U_0. Inserting (3.27) into (3.26), the equation for h_0 can be written

$$2d^{1/2}\frac{\partial h_0}{\partial X} + 3d^{-1}h_0\frac{\partial h_0}{\partial r} + \frac{d}{3}\frac{B^2}{A}\frac{\partial^3 h_0}{\partial r^3} + \frac{1}{2d^{1/2}}h_0\frac{\partial d}{\partial X} + \frac{d}{A}\left(\frac{C}{B}\right)^2\left[\frac{\partial\tilde{v_0}}{\partial y} + \frac{\partial\theta}{\partial Y}\left(\frac{\partial h_0}{\partial y} + \frac{\partial h_0}{\partial r}\frac{\partial\theta}{\partial Y}\right)\right] = \frac{1}{A}(\Omega_0 - \underline{\Omega}_0). \tag{3.29}$$

If we take the derivative of this equation with respect to r and use (3.6), we obtain the generalized KP equation:

$$\frac{\partial}{\partial r}\left(2d^{1/2}\frac{\partial h_0}{\partial X} + 3d^{-1}h_0\frac{\partial h_0}{\partial r} + \frac{d}{3}\frac{B^2}{A}\frac{\partial^3 h_0}{\partial r^3} + \frac{1}{2d^{1/2}}h_0\frac{\partial d}{\partial X}\right) + \frac{d}{A}\left(\frac{C}{B}\right)^2\left[\frac{\partial^2 h_0}{\partial y^2} + 2\frac{\partial\theta}{\partial Y}\frac{\partial h_0}{\partial r\partial y} + \frac{\partial^2 h_0}{\partial r^2}\left(\frac{\partial\theta}{\partial Y}\right)^2\right] = \frac{1}{A}\frac{\partial\Omega_0}{\partial r}. \tag{3.30}$$

Setting $\Omega_0 = 0$ provides an equation equivalent to that of Johnson (1983).

https://doi.org/10.1017/S0022112097005442 Published online by Cambridge University Press

We now examine the boundary layer to obtain the bottom boundary conditions on the averaged outer flow variables and an explicit relation for the flow due to displacement thickness.

4. Bottom boundary layer

The dimensionless boundary layer thickness is $A\epsilon^3/B$ as can be seen, for example, by examining the right-hand side of the turbulent stress equations in §2. Consequently, we introduce the boundary layer coordinate

$$Z = \frac{B\,(z+d)}{A\epsilon^3}, \tag{4.1}$$

and the boundary layer variables

$$u = \mathscr{U},\ \ v = \mathscr{V},\ \ w = \frac{A}{B}\epsilon^3 W,\ \ p = P,\ \ q = Q,\ \ \lambda = \frac{A}{B}\epsilon^3 L,\ \ \boldsymbol{\tau} = \boldsymbol{T}. \tag{4.2}$$

With the new coordinate and variables, the governing equations in the boundary layer with $O\left(\epsilon^3\right)$ errors are

$$\frac{\partial \mathscr{U}}{\partial r} d^{-1/2} + \frac{\partial W}{\partial Z} = 0, \tag{4.3}$$

$$-\frac{\partial \mathscr{U}}{\partial r} + \frac{\partial P}{\partial r} d^{-1/2} = \epsilon \frac{\partial T_{zx}}{\partial Z}, \tag{4.4}$$

$$\frac{\partial P}{\partial Z} = 0, \tag{4.5}$$

$$-\frac{\partial T_{zx}}{\partial r} + \frac{T_{zz}}{\epsilon}\frac{\partial \mathscr{U}}{\partial Z} = c_1 \frac{\partial}{\partial Z}\left(QL\frac{\partial T_{zx}}{\partial Z}\right) - \frac{Q}{L}T_{zx}, \tag{4.6}$$

$$-\frac{\partial T_{zz}}{\partial r} = c_1 \frac{\partial}{\partial Z}\left(QL\frac{\partial T_{zz}}{\partial Z}\right) - \frac{Q}{L}\left(T_{zz} + \frac{Q^3}{4}\right), \tag{4.7}$$

$$-\frac{\partial Q^2}{\partial r} = \frac{2}{\epsilon}T_{zx}\frac{\partial \mathscr{U}}{\partial Z} + c_1 \frac{\partial}{\partial Z}\left(QL\frac{\partial Q^2}{\partial Z}\right) - \frac{Q^3}{4L}, \tag{4.8}$$

$$-\frac{\partial L}{\partial r} + \frac{c_3 L}{\epsilon Q^2}T_{zx}\frac{\partial \mathscr{U}}{\partial Z} = c_1 \frac{\partial}{\partial Z}\left(QL\frac{\partial L}{\partial Z}\right) + c_2 Q - \frac{c_4}{Q}\left(\frac{\partial QL}{\partial Z}\right)^2, \tag{4.9}$$

with the boundary conditions

$$\mathscr{U} \to s_x\left(\Upsilon + \frac{\epsilon}{\kappa}\ln Z\right), \quad W \to -\epsilon B \mathscr{U}\frac{\partial d}{\partial X}, \tag{4.10}$$

$$T_{zx} \to |s_x|\,s_x, \quad T_{zz} \to -2^{1/2}s_x^2, \quad Q \to |s_x|, \quad L \to c_5 Z, \tag{4.11}$$

as $Z \to 0$. The equations for $\mathscr{V}$ are decoupled from this set.

After expanding in powers of ϵ and equating like-ordered terms, we find from the zeroth-order turbulence equations that $\mathscr{U}_0$ is independent of Z. (This is also the case for $\mathscr{V}_0$.) Therefore,

$$\mathscr{U}_0 = \Upsilon s_x^{(0)} = u_0 = \frac{h_0}{d^{1/2}} + U_0, \quad W_0 = -\frac{Z}{d}\frac{\partial h_0}{\partial r}, \quad P_0 = p_0 = H_0 + h_0. \tag{4.12}$$

Since the outer solution for $\tau_{zx}^{(0)}$ is independent of r and y, $\tau_{zx}^{(0)}$ tends to $\langle \underline{T_{zx}^{(0)}} \rangle$ in the

https://doi.org/10.1017/S0022112097005442 Published online by Cambridge University Press

limit $Z \to \infty$. Averaging the $O(\epsilon)$ x-momentum equation over r and y shows that $\langle \underline{T_{zx}^{(0)}} \rangle$ is independent of Z which with the boundary condition (4.11) means that

$$\langle \underline{T_{zx}^{(0)}} \rangle = \langle \underline{|s_x^{(0)}|\, s_x^{(0)}} \rangle, \tag{4.13}$$

throughout the boundary layer. Next, we can eliminate $\mathscr{U}_1$ from the continuity and momentum equations and solve for W_1 to obtain

$$W_1 = d^{-1/2} \left(T_{zx}^{(0)} - |s_x^0|\, s_x^0 \right) - \frac{Z}{d} \frac{\partial h_1}{\partial r} - B u_0 \frac{\partial d}{\partial X}. \tag{4.14}$$

If we match with the outer w using Van Dyke's matching rules, we find that

$$\Omega_0 = \frac{A}{B d^{1/2}} \left(\langle \underline{T_{zx}^{(0)}} \rangle - |s_x^0|\, s_x^0 \right) = \frac{A}{B \Upsilon^2 d^{1/2}} \left(\langle \underline{|u_0|\, u_0} \rangle - |u_0|\, u_0 \right), \tag{4.15}$$

whereby

$$\langle \underline{\Omega_0} \rangle = 0. \tag{4.16}$$

Now by analogy with the laminar oscillatory boundary layer theory of Stuart (1966) and with a very similar problem discussed by Jacobs (1990) in which he used a different turbulence model, we let

$$\mathscr{U}_1 = f(r, y, X, Y) + F(r, y, X, Y, Z), \tag{4.17}$$

where f solves

$$-\frac{\partial f}{\partial r} + d^{-1/2} \frac{\partial h_1}{\partial r} = 0, \quad \underline{f} = 0, \tag{4.18}$$

and the periodic parts of F decay exponentially as we go out of the boundary layer. Consequently, by using the method of intermediate equations (Van Dyke 1975, p. 225–226), the boundary conditions at the outer edge of the boundary layer for F and the zeroth-order turbulence quantities are

$$F \to \tilde{\mu} + \frac{|M|^{1/2} \operatorname{sgn}(M)}{\kappa} \ln Z,$$

$$T_{zx}^{(0)} \to M, \quad T_{zz}^{(0)} \to -2^{1/2} |M|, \quad Q_0 \to 2^{5/4} |M|^{1/2}, \quad L_0 \to c_5 Z, \tag{4.19}$$

as $Z \to \infty$, where $\tilde{\mu}$ and M are only functions of X and Y since equation (4.19) is an exact solution of the boundary layer equations if the variables are independent of r and y. At this stage, $\tilde{\mu}$ is undetermined; but, from (4.12), (4.13), and (4.19), we have

$$M = \langle \underline{|s_x^{(0)}|\, s_x^{(0)}} \rangle = \frac{\langle \underline{|u_0|\, u_0} \rangle}{\Upsilon^2}. \tag{4.20}$$

Following a similar procedure at the next order, we obtain

$$\langle \underline{\Omega_1} \rangle = 0. \tag{4.21}$$

Since we have the form of the boundary conditions at the outer edge of the boundary layer, simple matching provides the boundary conditions for the outer variables in terms of the outer coordinates. At this stage, we have all the necessary elements to close the equations.

5. Closing the equations

To simplify notation, let us omit subscripts on the lowest-order surface elevation. Similarly, we will omit superscripts on the lowest-order stress components, turbulent

https://doi.org/10.1017/S0022112097005442 Published online by Cambridge University Press

kinetic energy, and turbulent macroscale. Using (4.16), we see from (3.28) that we must have

$$\frac{\partial}{\partial X}\left(U_0 \mathrm{d}\right) = 0, \tag{5.1}$$

which after use of the initial condition (2.35) yields

$$U_0 = 0. \tag{5.2}$$

Integration of the $O\left(\epsilon^5\right)$ outer continuity equation over the depth, averaging over r and y, and using (4.21) gives

$$\frac{\partial}{\partial X}\int_{-d}^{0} U_1 \mathrm{d}z = 0. \tag{5.3}$$

The initial condition (2.35) applied to this equation requires that

$$\int_{-d}^{0} U_1 \mathrm{d}z = 0, \tag{5.4}$$

which provides the extra equation to determine $\tilde{\mu}$ in (4.19).

Equation (3.27) yields a relation for the lowest-order r-averaged velocity in the y-direction,

$$\frac{\partial V_0}{\partial y} = \frac{BA}{C^2\Upsilon^2 d^{5/2}}\left[\langle \underline{|h|\, h}\rangle - \underline{|h|\, h}\right], \tag{5.5}$$

where we also have used (5.2), (4.15), and (3.6). In order to solve for V_0 unambiguously, we impose the condition $\langle V_0\rangle = 0$ since there are no Stokes drift effects at this order and there is no mean forcing in the y-direction (i.e. no mean surface tilt in the y-direction) at this order. This boundary condition is also consistent with (2.35).

Applying equation (3.23) at $z = -d$ and using the boundary condition on the shear stress (see equations (4.19) and (4.20)), we obtain

$$\frac{\partial H}{\partial X} = -\frac{\langle \underline{|h|\, h}\rangle}{Bd^2\Upsilon^2}, \tag{5.6}$$

which is an equation governing the setdown of the waves.

Using (4.15), our elevation equation (3.31) becomes

$$\frac{\partial}{\partial r}\left(\frac{\partial h}{\partial X} + \frac{3}{2}d^{-3/2}h\frac{\partial h}{\partial r} + \frac{d^{1/2}}{6}\frac{B^2}{A}\frac{\partial^3 h}{\partial r^3} + \frac{h}{4d}\frac{\partial d}{\partial X} + \frac{|h|\, h}{2Bd^2\Upsilon^2}\right)$$

$$+ \frac{d^{1/2}}{2A}\left(\frac{C}{B}\right)^2\left[\frac{\partial^2 h}{\partial y^2} + 2\frac{\partial \theta}{\partial Y}\frac{\partial h}{\partial r\partial y} + \frac{\partial^2 h}{\partial r^2}\left(\frac{\partial \theta}{\partial Y}\right)^2\right] = 0. \tag{5.7}$$

Given an initial form for h at $x = 0$ and (3.24), we have all the information needed to solve (5.7). Having obtained h, we can find H and V_0 using (5.6) and (5.5).

As mentioned in §3, setting the turbulent dissipation term equal to zero reproduces an equation given by Johnson (1983). Eliminating all y and Y variations reproduces an equation derived by Jacobs (1997), and eliminating all depth variations as well as the dissipative term recovers the inviscid model of Segur & Finkel (1985).

The equations governing the lowest-order turbulence quantities and U_1 are (5.4) and

$$\tau_{zz}\frac{\partial U_1}{\partial z} = c_1\frac{\partial}{\partial z}\left(q\lambda\frac{\partial \tau_{zx}}{\partial z}\right) - \frac{q}{\lambda}\tau_{zx}, \tag{5.8}$$

https://doi.org/10.1017/S0022112097005442 Published online by Cambridge University Press

$$c_1 \frac{\partial}{\partial z}\left(q\lambda \frac{\partial \tau_{zz}}{\partial z}\right) = \frac{q}{\lambda}\left(\tau_{zz} + \frac{q^2}{4}\right), \tag{5.9}$$

$$2\tau_{zx}\frac{\partial U_1}{\partial z} + c_1 \frac{\partial}{\partial z}\left(q\lambda \frac{\partial q^2}{\partial z}\right) = \frac{q^3}{4\lambda}, \tag{5.10}$$

$$\frac{c_3\lambda}{q^2}\tau_{zx}\frac{\partial U_1}{\partial z} = c_1 \frac{\partial}{\partial z}\left(q\lambda \frac{\partial \lambda}{\partial z}\right) + c_2 q - \frac{c_4}{q}\left[\frac{\partial}{\partial z}(q\lambda)\right]^2, \tag{5.11}$$

with

$$\frac{\partial \tau_{zz}}{\partial z} = \frac{\partial q}{\partial z} = \frac{\partial \lambda}{\partial z} = 0, \tag{5.12}$$

at $z = 0$,

$$U_1 \to \mu + \frac{|M|^{1/2}\operatorname{sgn}|M|}{\kappa}\ln\left(\frac{z+d}{d}\right),$$

$$T_{zx} \to M, \quad T_{zz} \to -2^{1/2}|M|, \quad Q \to 2^{5/4}|M|^{1/2}, \quad \lambda \to c_5 Z, \tag{5.13}$$

as $z \to -d$, where

$$M = \frac{\langle |h|\, h\rangle}{d\Upsilon^2}. \tag{5.14}$$

Thus after finding h, (5.4) and (5.8)–(5.14) provide a closed system to obtain U_1 and the turbulence quantities. We will now discuss our methods of solving these equations and the behaviour of the solutions.

6. Numerical solution

We shall restrict our attention to topography contours which are plane and parallel to the y-axis. Although this topography is simple, it approximates many natural beaches; later efforts will explore more complicated topographical configurations. It proves convenient to rewrite the evolution equation and setdown equation in terms of the original parameters α, δ_x, δ_y, and γ_x. Therefore if the depth is described by $d = (1 - \gamma_x x)^{1/2}$, then the evolution equation (5.7) can be simplified for this special case to

$$\frac{\partial}{\partial r}\left(\frac{\partial h}{\partial x} + \frac{3\alpha}{2d^{3/2}}h\frac{\partial h}{\partial r} + \frac{\delta_x^2 d^{1/2}}{6}\frac{\partial^3 h}{\partial r^3} + \frac{h\gamma_x}{4d} + \frac{\alpha\epsilon^2}{2\delta_x d^2\Upsilon^2}|h|\, h\right) + \frac{d^{1/2}}{2}\left(\frac{\delta_y}{\delta_x}\right)^2\frac{\partial^2 h}{\partial y^2} = 0, \tag{6.1}$$

while the equation for the setdown (5.6) and the x-derivative of the first equation in (3.1) can be written

$$\frac{\partial H}{\partial x} = -\frac{\alpha\epsilon^2}{\delta_x d^2\Upsilon^2}\langle |h|\, h\rangle, \quad \frac{\partial r}{\partial x} = (d + \alpha H)^{-1/2}. \tag{6.2}$$

The initial conditions at $x = 0$ are

$$h = \Xi(r, y), \quad r = -t, \quad H = 0, \tag{6.3}$$

where Ξ, the offshore wave elevation, is assumed to be known and is a zero-mean periodic function of both its arguments.

https://doi.org/10.1017/S0022112097005442 Published online by Cambridge University Press

Many authors have integrated the KP equation in a variety of applications (*e.g.* Katsis & Akylas 1987 and Mathew & Akylas 1990). Since our problem is periodic in two spatial dimensions, we have chosen to solve the evolution equation using a Fourier method in both r and y and centred finite differencing in the marching variable x. If we define

$$r_k = \frac{k\pi}{N_r}, \quad 0 \leqslant k \leqslant 2N_r - 1, \tag{6.4}$$

$$y_l = \frac{l\pi}{N_y}, \quad 0 \leqslant l \leqslant 2N_y - 1, \tag{6.5}$$

$$b_k = \begin{cases} 2, & k = \pm N_r \\ 1, & k \neq \pm N_r \end{cases}, \quad c_k = \begin{cases} 2, & l = \pm N_y \\ 1, & l \neq \pm N_y \end{cases}, \tag{6.6}$$

$$f(r, y) = \sum_{k=-N_r}^{N_r} \sum_{l=-N_y}^{N_y} \frac{\hat{f}(k, l)}{b_k c_l} \mathrm{e}^{\mathrm{i}(kr+ly)}, \tag{6.7}$$

$$\hat{f}(k, l) = \frac{1}{4N_r N_y} \sum_{j=0}^{2N_r-1} \sum_{m=0}^{2N_y-1} f\left(r_j, y_m\right) \mathrm{e}^{-\mathrm{i}\left(kr_j+ly_m\right)}, \tag{6.8}$$

then the equation for $\hat{h}$ when $k \neq 0$ is

$$\frac{\partial \hat{h}}{\partial x} + \frac{\gamma_x}{4d}\hat{h} - \frac{\delta_x^2 d^{1/2}}{6}\mathrm{i}k^3\hat{h} + \frac{d^{1/2}}{2}\left(\frac{\delta_y}{\delta_x}\right)^2 \frac{\mathrm{i}l^2}{k}\hat{h} = \frac{-\mathrm{i}}{k}\hat{F}, \tag{6.9}$$

where

$$F = -\frac{3\alpha}{2d^{3/2}}\frac{\partial}{\partial r}\left(h\frac{\partial h}{\partial r}\right) - \frac{\alpha\epsilon^2}{2\delta_x d^2 \Upsilon^2}\frac{\partial}{\partial r}|h|\, h. \tag{6.10}$$

For $k = 0$, we will require that $\hat{h} = 0$. This corresponds to $\underline{h} = 0$ and is analogous to the normalization condition of Segur & Finkel (1985) or that discussed by Grimshaw & Melville (1989); it also satisfies our initial condition at $x = 0$ (equation (2.35)).

Defining an incremental step in x as Δx and letting $x_n = n(\Delta x)$ $(n = 0, 1 \ldots)$, we evaluate the terms on the left of equation (6.9) implicitly, and evaluate the nonlinear terms, $\hat{F}$, explicitly. In calculating the nonlinear terms, the multiplies are calculated in physical space while the derivatives are calculated in spectral space. For the first step, we use backward Euler; centred finite differencing is used thereafter. Thus for $n > 0$,

$$\hat{h}_{n+1} = \frac{(1 - \Delta x L_{n-1})\,\hat{h}_{n-1} + 2\Delta x \hat{F}_n}{(1 + \Delta x L_{n+1})}, \tag{6.11}$$

where

$$L_n = \left(\frac{\gamma_x}{4d} - \frac{\delta_x^2 d^{1/2}}{6}\mathrm{i}k^3 + \frac{d^{1/2}}{2}\left(\frac{\delta_y}{\delta_x}\right)^2 \frac{\mathrm{i}l^2}{k}\right)\Bigg|_{x=x_n}. \tag{6.12}$$

Once $\hat{h}$ has been calculated, we use an inverse FFT to find $h(x, r, y)$. Everywhere the FFT was used, we exploited the reality of h to avoid redundant calculations (Cooley, Lewis & Welch 1970).

Since we have couched this study as a signalling wave problem (i.e. one in which waves are continually generated at a given location as opposed to examining the time evolution of one wave), it is sufficient to plot h at any convenient time. At a fixed

https://doi.org/10.1017/S0022112097005442 Published online by Cambridge University Press

time, r is a unique function of x as can be seen in the first of the equations in (3.1). The new h and the h at the previous step can be used to advance H and r using the trapezoidal rule

$$g_{n+1} = g_n + \frac{\Delta x}{2}(G_{n+1} + G_n), \tag{6.13}$$

where g is H or r, and G is the corresponding right-hand side of (6.2). Once r is found at the new x, we use the interpolation polynomial given in Gottlieb, Hussaini, & Orszag (1984) to provide h as a function of only x and y at a given time t. In the figures below, we have chosen to display $h(x, y)$ at $t = 0$.

The system (5.4), (5.8–5.14) can be written in canonical form which allows us to avoid calculating this system at each cross-shore position. If we define the coordinate

$$Z = \frac{z + d}{d}, \tag{6.14}$$

and the variables

$$\Gamma = \frac{U_1 - \mu}{|M|^{1/2}\mathrm{sgn}(M)}, \quad T_{zx} = \frac{\tau_{zx}}{M}, \quad T_{zz} = \frac{\tau_{zz}}{|M|}, \quad Q = \frac{q}{|M|^{1/2}}, \quad \Lambda = \frac{\lambda}{d}, \tag{6.15}$$

then the shear stress is

$$T_{zx} = 1 - Z, \tag{6.16}$$

and the equations are

$$\frac{\mathrm{d}\Gamma}{\mathrm{d}Z} = -\frac{1}{T_{zz}}\left[c_1\frac{\mathrm{d}(Q\Lambda)}{\mathrm{d}Z} + \frac{Q}{\Lambda}(1 - Z)\right], \tag{6.17}$$

$$c_1\frac{\mathrm{d}}{\mathrm{d}Z}\left(Q\Lambda\frac{\mathrm{d}T_{zz}}{\mathrm{d}Z}\right) = \frac{Q}{\Lambda}\left(T_{zz} + \frac{Q^2}{4}\right), \tag{6.18}$$

$$c_1\frac{\mathrm{d}}{\mathrm{d}Z}\left(Q^2\Lambda\frac{\mathrm{d}Q}{\mathrm{d}Z}\right) = \frac{Q^3}{8\Lambda} - (1 - Z)\frac{\mathrm{d}\Gamma}{\mathrm{d}Z}, \tag{6.19}$$

$$c_1\frac{\mathrm{d}}{\mathrm{d}Z}\left(Q\Lambda\frac{\mathrm{d}\Lambda}{\mathrm{d}Z}\right) = -c_2 Q + \frac{c_3\Lambda}{Q^2}(1 - Z)\frac{\mathrm{d}\Gamma}{\mathrm{d}Z} + \frac{c_4}{Q}\left[\frac{\mathrm{d}(Q\Lambda)}{\mathrm{d}Z}\right]^2, \tag{6.20}$$

with the boundary conditions

$$\frac{\mathrm{d}}{\mathrm{d}Z}(T_{zz}, Q, \Lambda) = 0, \tag{6.21}$$

at $Z = 1$, and

$$\Gamma \to \frac{1}{\kappa}\ln Z, \quad T_{zz} \to -2^{1/2}, \quad Q \to 2^{5/4}, \quad \Lambda \to c_5 Z, \tag{6.22}$$

as $Z \to 0$. This defines a standard two-point boundary value problem for which there exist several high-quality solvers. We chose to use the routine COLNEW developed by Ascher and colleagues (see Ascher, Christiansen & Russell 1981; Bader & Ascher 1987; and Ascher, Mattheij & Russell 1988) which is available on NETLIB. Once Γ has been found, the additive function μ can be obtained by using equations (5.4) and (6.15) and is given by

$$\mu = -|M|^{1/2}\mathrm{sgn}(M)\int_0^1 \Gamma \, \mathrm{d}Z. \tag{6.23}$$

https://doi.org/10.1017/S0022112097005442 Published online by Cambridge University Press

The accuracy of the mean flow calculation is monitored by providing COLNEW with tolerances on the dependent variables (set to about 10^{-14}). With the bottom boundary condition applied at $Z = 0.01$, we found

$$\int_0^1 \Gamma \, \mathrm{d}Z = -2.32. \tag{6.24}$$

The equation for V_0 (5.6) can be written

$$\frac{\partial V_0}{\partial y} = \frac{\alpha \delta_x \epsilon^2}{\delta_y^2 \Upsilon^2 d^{5/2}} \left(\langle |\underline{h}| \, h \rangle - |\underline{h}| \, h \right), \tag{6.25}$$

with the boundary condition discussed in §5. Hence, we have

$$V_0 = \int^y \frac{\alpha \delta_x \epsilon^2}{\delta_y^2 \Upsilon^2 d^{5/2}} \left(\langle |\underline{h}| \, h \rangle - |\underline{h}| \, h \right) \mathrm{d}y' + g(X), \tag{6.26}$$

where g can be found by requiring the y-average of V_0 to be zero. We calculated V_0 by using the Fourier coefficients of the integrand (see Appendix B).

7. Discussion

In the calculations, we typically used $N_x = N_y = 64$ with $\Delta x = 0.001$; these values provided satisfactory accuracy. Following Jacobs (1990, 1997), we took Υ equal to 1 in all cases. The other parameter values used in the numerical experiments were $\alpha = 0.09$, $\delta_x = 0.3$, $\delta_y = 0.09$, $\gamma_x = 0.0125$, and $\epsilon = 0.2$. This gives a drag coefficient of 0.04 and a bottom slope of 0.00375. For water of depth 3 m, the parameters correspond to a initial period of 11.6 s and a sinusoidal wave with peak-to-trough height of 27 cm. (Smaller drag coefficients provided qualitatively similar results except that the region of substantial wave decay was shifted toward smaller depths.) Five different initial profiles were used (see figure 2*a–e*, all have $\langle \underline{h}^2 \rangle = 0.125$):

(1) a genus 1 solution of the inviscid flat-bottomed KP equation (a cnoidal wave). $\mu = 1$, $\nu = 1$, and $b = -3.5208$ in the notation of Segur & Finkel (1985) (see also Appendix C);

(2) $\frac{1}{2} \sin(r + y)$;

(3) a symmetric (terminology of Hammack *et al.* 1989) genus 2 solution of the inviscid flat-bottomed KP equation. $\mu_1 = 1$, $\mu_2 = 1$ $\nu_1 = -1$, $\nu_2 = 1$, $b = -3.7372$, $d = -3.7372$, and $\lambda = 1/2$ in the notation of Segur & Finkel (1985) (see also Appendix C);

(4) $(1/\sqrt{2}) \sin(r) * \sin(y)$;

(5) an asymmetric (terminology of Hammack *et al.* 1995) genus 2 solution of the inviscid flat-bottomed KP equation. $\mu_1 = 1$, $\mu_2 = 1$ $\nu_1 = -1$, $\nu_2 = 0$, $b = -3.7372$, $d = -3.7372$, and $\lambda = 1/2$ in the notation of Segur & Finkel (1985) (see also Appendix C).

We see from figures 3 and 4 that initially planar waves remain planar (i.e. initially straight-crested waves remain straight crested as they approach the shore); these solutions are rotated versions of those obtained from the damped KdV equation derived by Jacobs (1997). Thus, as in Jacobs's paper, the sinusoidal initial profile (case 2) develops strong secondary peaks at shallow depths and resembles trains of polycnoidal waves discussed by Boyd (1990). In contrast, the cnoidal initial profile (case 1) evolves into a sequence of solitary waves. By using linear wave theory, we would expect wavelengths to shorten and would expect straight crested waves to

https://doi.org/10.1017/S0022112097005442 Published online by Cambridge University Press

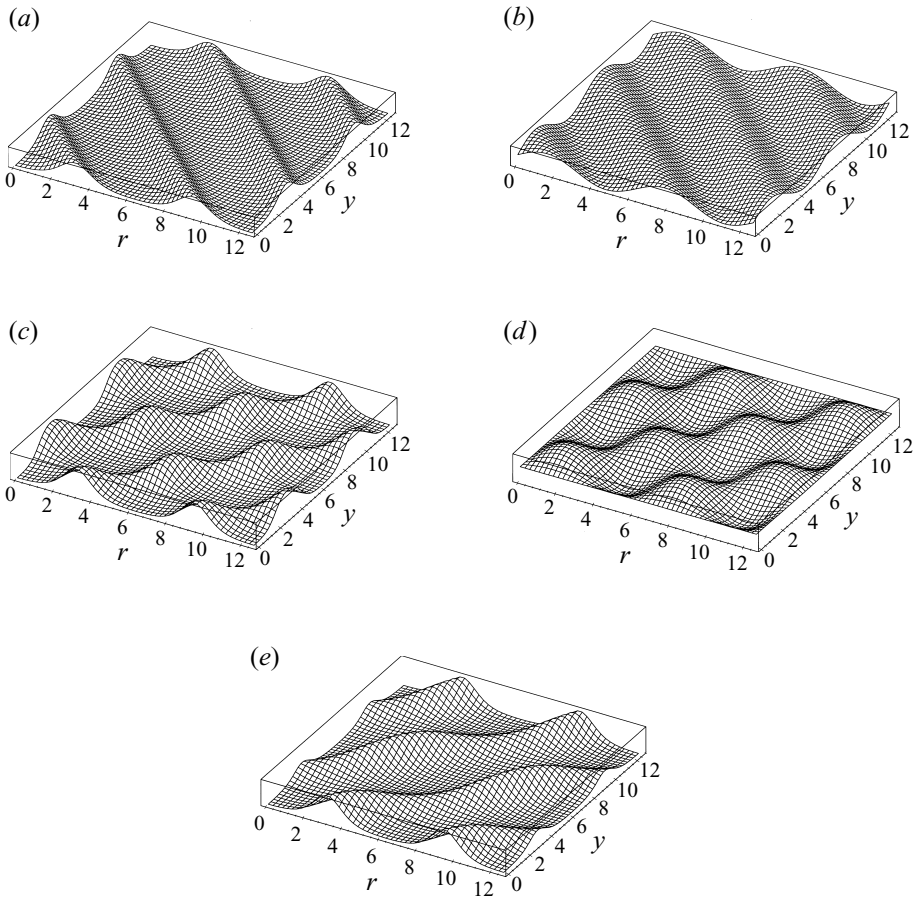


FIGURE 2. Initial wave profiles $h(r, y)$ at $x = 0$: (*a*) case 1; (*b*) case 2; (*c*) case 3; (*d*) case 4; (*e*) case 5.

rotate toward an orientation parallel to the y-axis; from the contour plots, we can verify that this is also the case for our nonlinear waves. For all the cases examined, the trough region becomes shallower, and the width of the peaks becomes narrower as the depth decreases.

As discussed in Segur & Finkel (1985), the non-planar waves (see figures 5*d*, 6*d*, and 7*d*) have hexagonal surface patterns. We can see the hexagons best in the contour plots of cases 3 and 4; in case 5, the single hexagon (per period in y) is not centred on the y-domain. As the depth decreases, the acute included angles of the hexagons decrease and the x-distance between successive hexagons decreases. Hammack *et al.* (1991) mention that the hexagonal pattern in their experiments remained intact up to and past breaking but it is unclear whether their bottom boundary layer is turbulent; moreover, the laboratory bottom slope is an order of magnitude larger than ours. In all their experiments, the main focus was on the behaviour of the waves over a flat bottom. It would be interesting to examine the effect of topography on the hexagonal pattern in the laboratory.

Here, although the hexagons can be seen at all depths, they slowly change shape. At the shallowest depths, the patterns become more complicated by the addition of secondary peaks particularly with case 4 which was the non-planar case that did

https://doi.org/10.1017/S0022112097005442 Published online by Cambridge University Press

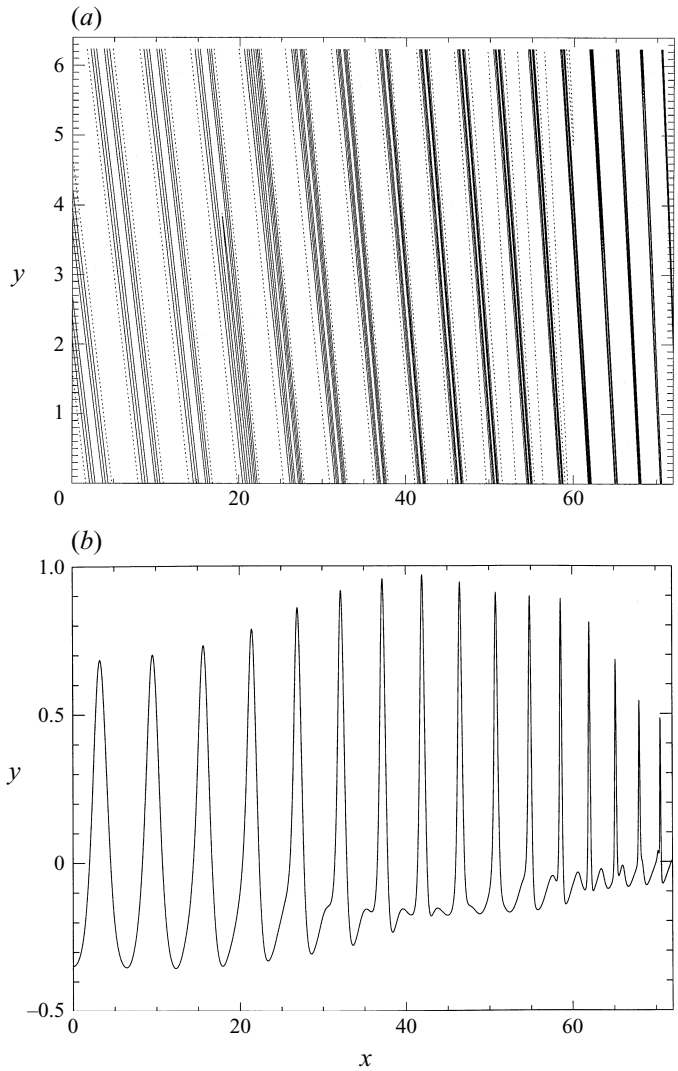


FIGURE 3. Case 1: (*a*) contour plot of $h(x, y, t = 0)$, dotted contours are negative-valued; (*b*) $h(x, y = 0, t = 0)$.

not initially solve the inviscid KP equation. This is analogous to the planar wave behaviour in which the sinusoid exhibited larger secondary peaks than the cnoidal wave. Nevertheless, as $d \to 0$, the initially sinusoidal-like waves show qualitatively similar asymptotic behaviour to the waves which initially solved the inviscid KP equation. In addition, although not shown here, we found that the plots of $\langle \underline{h^2} \rangle$ as a function of x, were similar for all the cases.

Figures 8 and 9 show typical plots of the mean surface level, αH, and the mean x-velocity, U_1, respectively. Since the bottom stress in the x-direction is always positive in the cases considered, a setdown occurs. Setdown values of this order of magnitude are observed outside of breaking; however, this mechanism for setdown is different than that of Longuet-Higgins & Stewart (1964) which is purely irrotational. From figure 9, we see that the mean x-velocity is positive (onshore) near the top and

https://doi.org/10.1017/S0022112097005442 Published online by Cambridge University Press

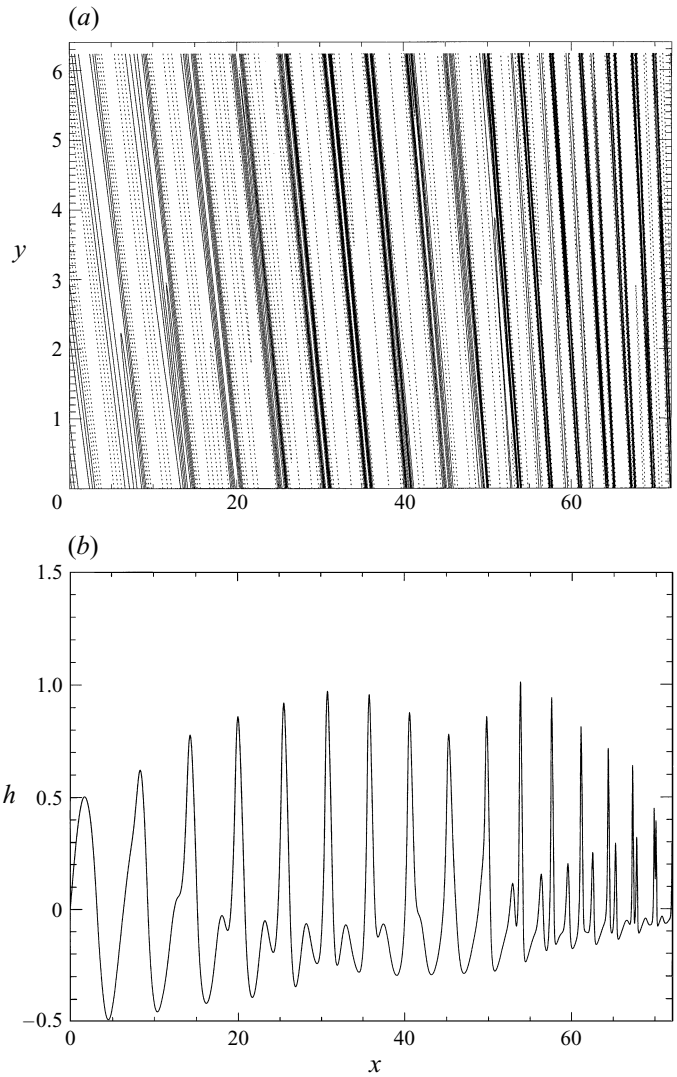


FIGURE 4. Case 2: (*a*) contour plot of $h(x, y, t = 0)$, dotted contours are negative-valued; (*b*) $h(x, y = 0, t = 0)$.

negative (offshore) near the bottom of the water column. Stokes drift effects would undoubtedly alter our profiles (since the depth-integrated mean cross-shore current would have to balance the depth-integrated Stokes drift for conservation of mass) but are not taken into account at this stage of our theory.

The initially planar waves did not generate a zeroth-order longshore current V_0; however, when the crests are curved, a non-zero V_0 does develop (see figures 5*e*, 6*e*, and 7*e*). Cases 3 and 4 produce a V_0 with two peaks and troughs while case 5 only displays one. This is related to the initial profiles which in case 5 only show one hexagon per period in y but in cases 3 and 4 show 2 hexagons. Usually in nearshore theories, longshore currents are assumed to be only generated by wave breaking; our theory predicts that small periodic longshore currents can develop outside areas of wave breaking due to turbulent bottom friction.

https://doi.org/10.1017/S0022112097005442 Published online by Cambridge University Press

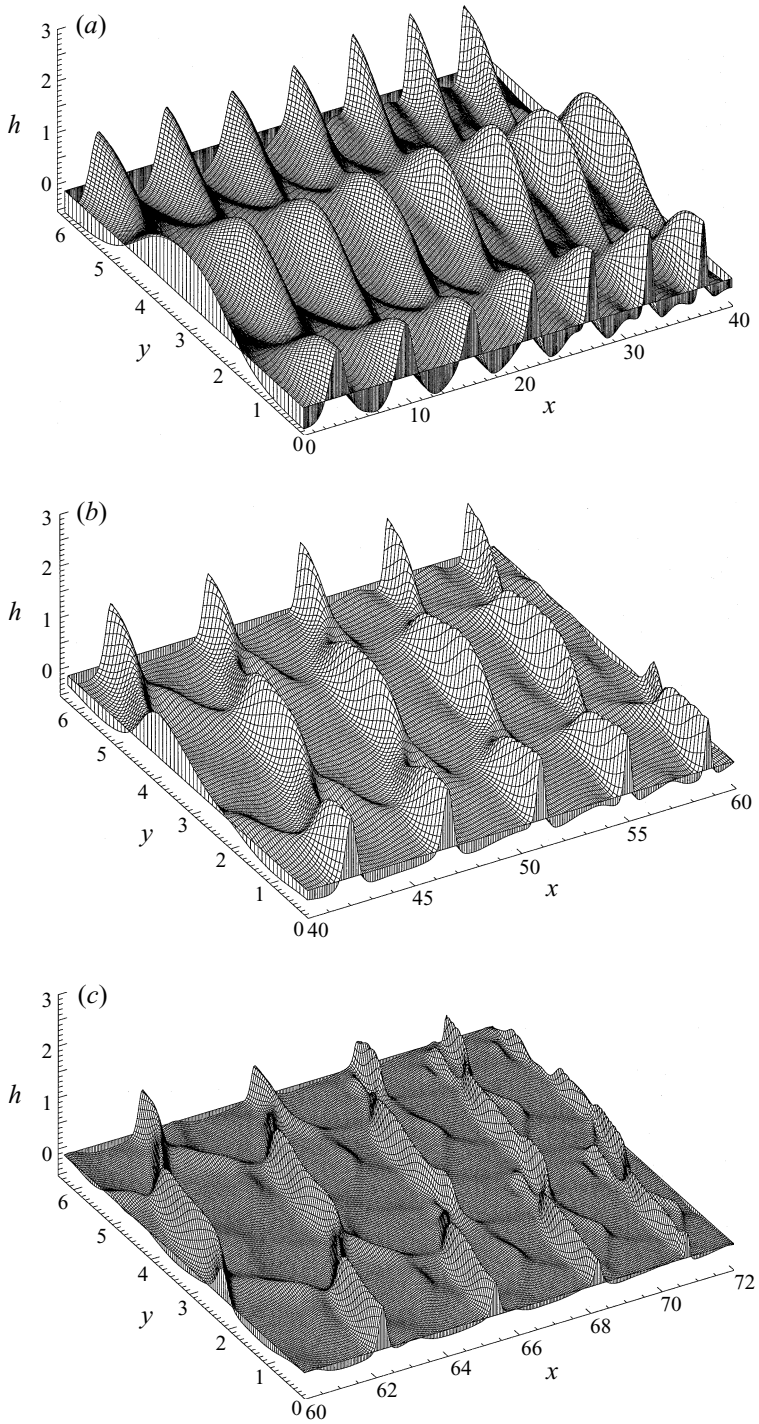


FIGURE 5(*a–c*). For caption see facing page.

https://doi.org/10.1017/S0022112097005442 Published online by Cambridge University Press

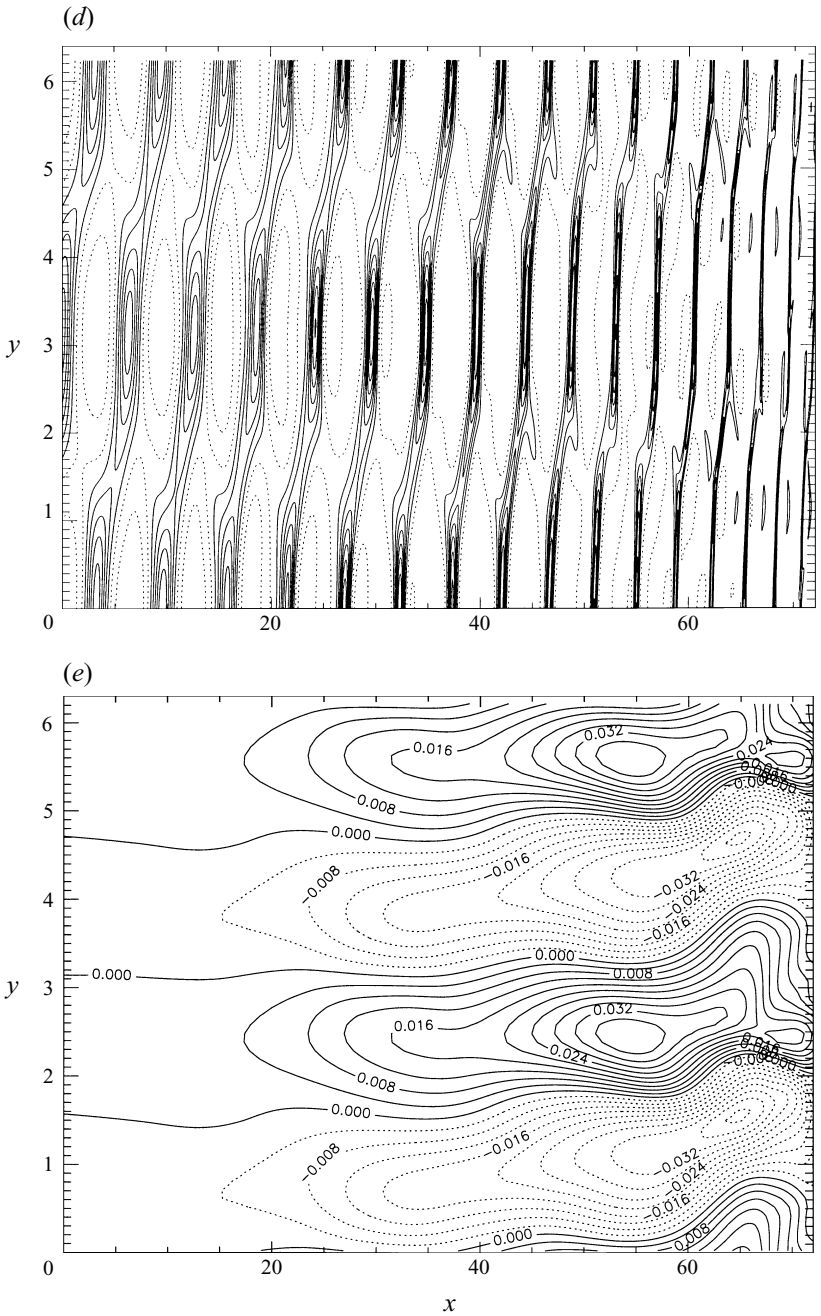


FIGURE 5. Case 3: (a, b, c) surface plots of $h(x, y, t = 0)$ at various depth ranges; (d) contour plot of $h(x, y, t = 0)$, dotted contours are negative-valued; (e) contour plot of V_0.

https://doi.org/10.1017/S0022112097005442 Published online by Cambridge University Press

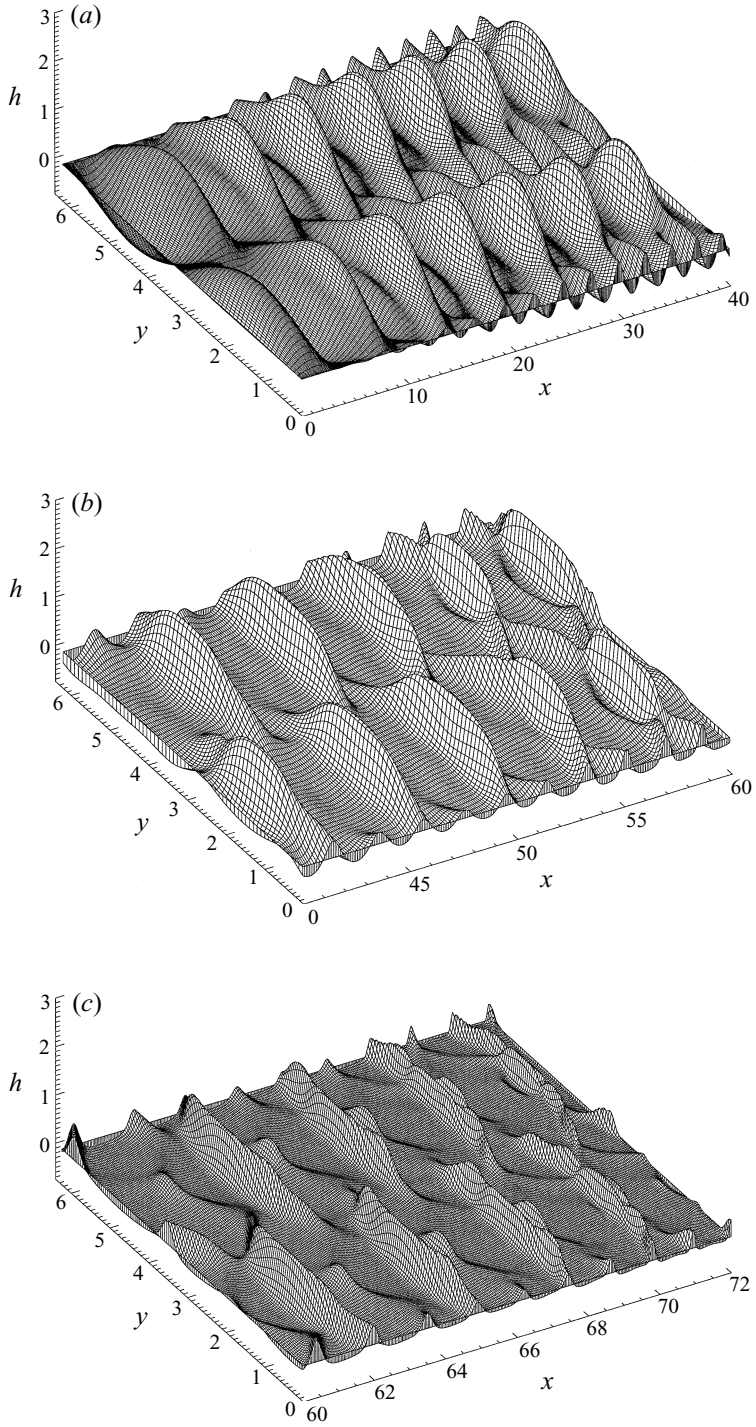


FIGURE 6(*a–c*). For caption see facing page.

https://doi.org/10.1017/S0022112097005442 Published online by Cambridge University Press

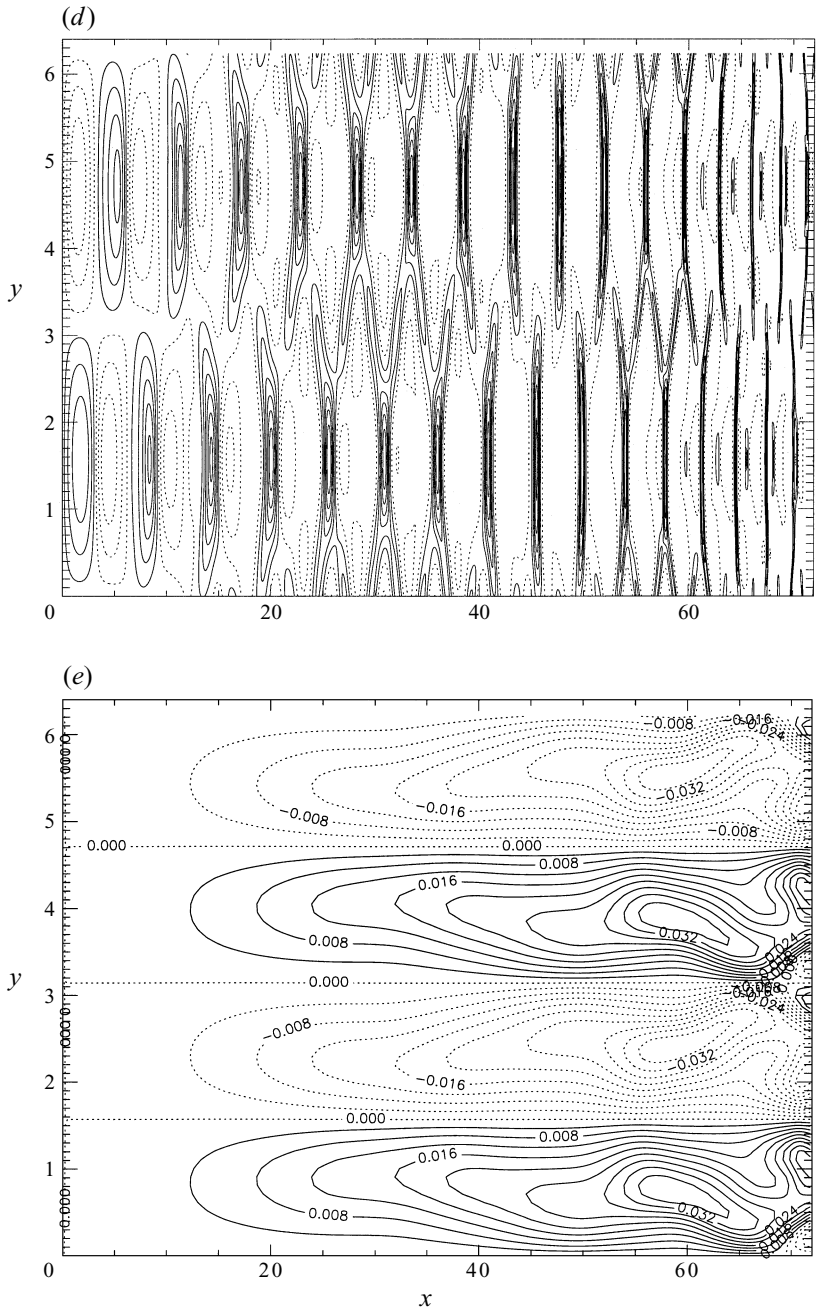


FIGURE 6. Case 4: (a, b, c) surface plots of $h(x, y, t = 0)$ at various depth ranges; (d) contour plot of $h(x, y, t = 0)$, dotted contours are negative-valued; (e) contour plot of V_0.

8. Concluding remarks

The purpose of this work was to include turbulent dissipation and variable-depth effects in a rational way to the ideal fluid model of Segur & Finkel (1985). In doing so, we extended the study of Jacobs (1997) by introducing two-dimensional effects and by calculating the currents generated by wave decay. Our theory is expected to

https://doi.org/10.1017/S0022112097005442 Published online by Cambridge University Press

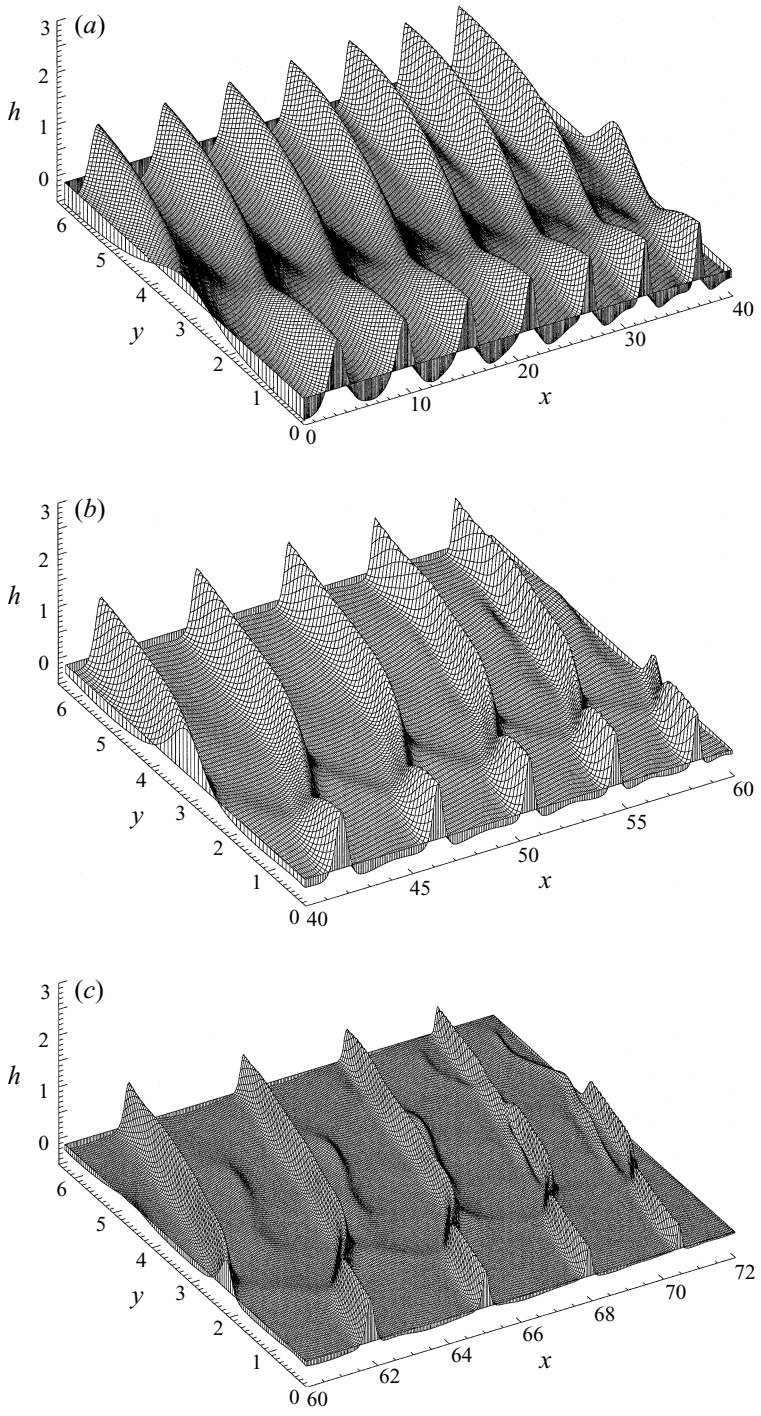


FIGURE 7(*a–c*). For caption see facing page.

https://doi.org/10.1017/S0022112097005442 Published online by Cambridge University Press

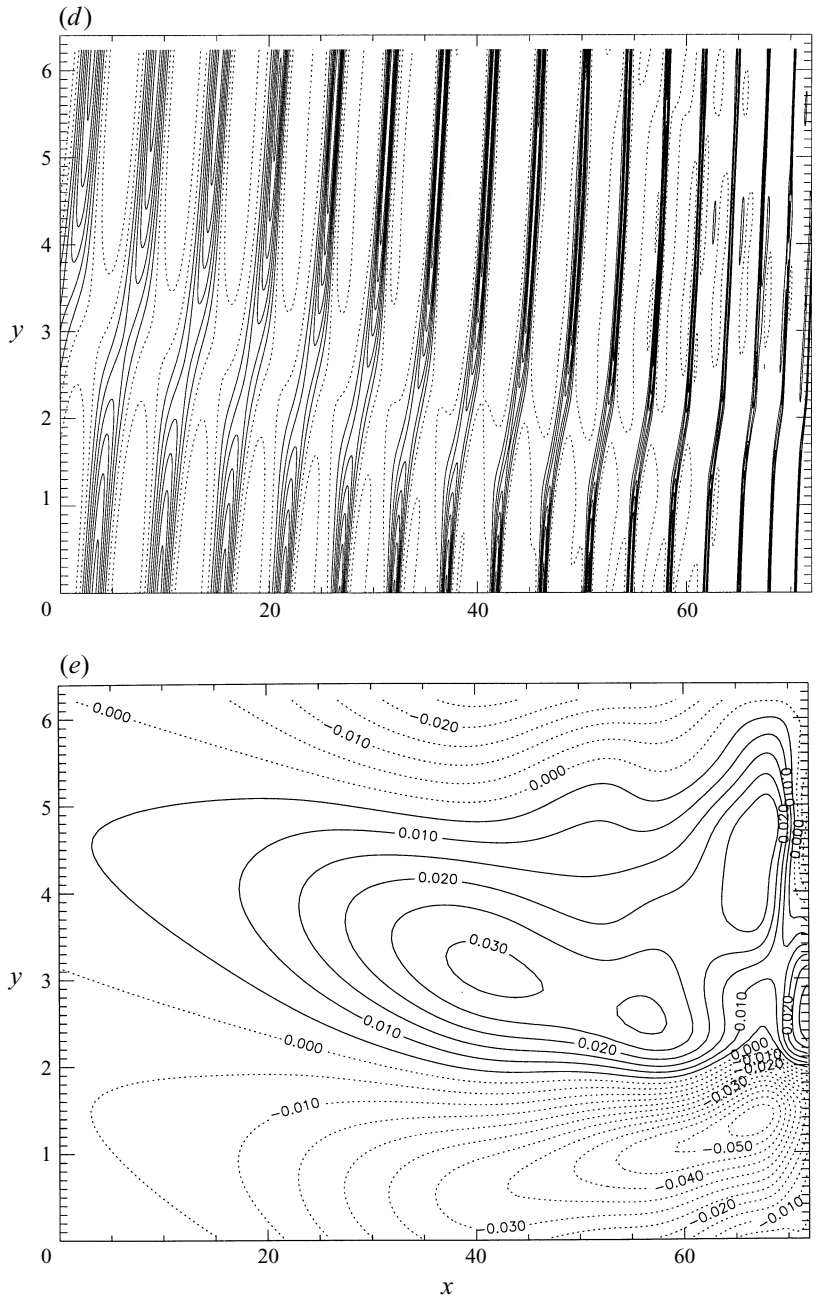


FIGURE 7. Case 5: (a, b, c) surface plots of $h(x, y, t = 0)$ at various depth ranges; (d) contour plot of $h(x, y, t = 0)$, dotted contours are negative-valued; (e) contour plot of V_0.

be valid for small-amplitude waves with weak dispersion, weak two-dimensionality, and weak dissipation in regions outside wave breaking and where bottom slopes are small.

In future efforts, we believe it would be interesting and worthwhile to extend our theory to a higher order so as to include Stokes drift effects and longshore variations

https://doi.org/10.1017/S0022112097005442 Published online by Cambridge University Press

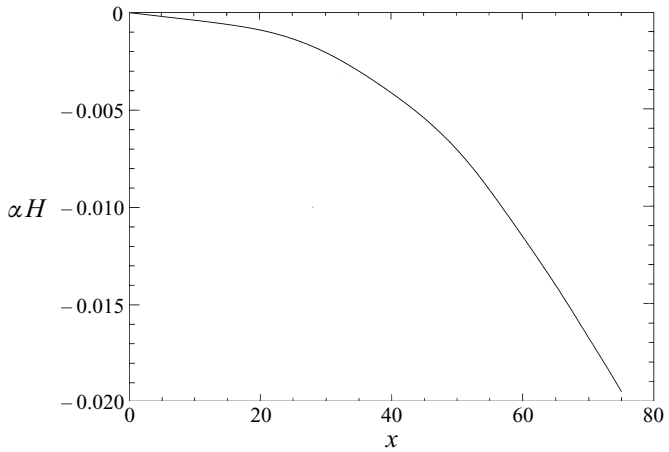


FIGURE 8. Case 3: the lowest-order setdown αH.

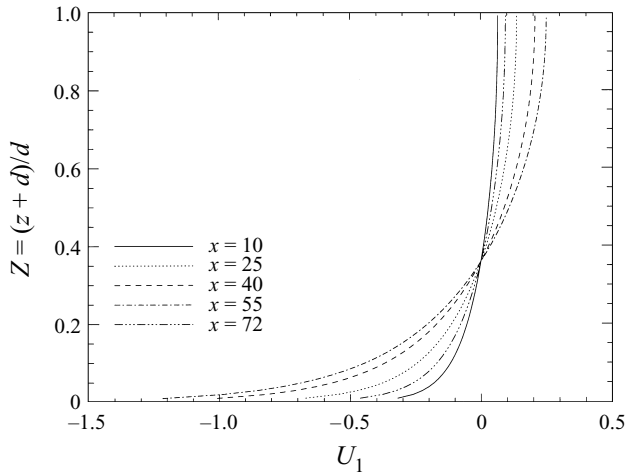


FIGURE 9. Case 3: the first-order mean x velocity U_1 at various cross-shore positions.

of the cross-shore current. Furthermore, other logical extensions of the theory might be to include wind stresses, wave breaking models, and larger bottom slopes. It also would be interesting to develop a turbulent generalization of the two-dimensional Boussinesq equations to allow the possibility of backward travelling waves. Finally, it is important to note, as Jacobs (1997) has explained in detail, that the dissipation term obtained from the flow due to displacement thickness is independent of the turbulence model (for models which give a logarithmic layer) to this order. However, the calculation of U_1 will vary slightly from model to model.

We are grateful to Professor John P. Boyd and Dr Beth A. Wingate for helpful comments on an earlier draft of this paper and to Professor Stanley J. Jacobs for a wealth of useful advice. This work was supported under the Program in Ocean Surface Processes and Remote Sensing at the University of Michigan, funded under the University Research Initiative of the Office of Naval Research, Contract No. N00014-92-J1650.

https://doi.org/10.1017/S0022112097005442 Published online by Cambridge University Press

Appendix A. Curvilinear coordinate systems

The definitions of the curvilinear unit vectors for the top surface $(\hat{\boldsymbol{S}}_1, \hat{\boldsymbol{S}}_2, \hat{\boldsymbol{N}})$ can be obtained using standard techniques (see Aris 1989, Chapter 7) from the coordinate system, (S_1, S_2, N), defined by

$$x = S_1 - \frac{N\partial\zeta/\partial S_1}{\Psi}, \quad y = S_2 - \frac{N\partial\zeta/\partial S_2}{\Psi}, \quad z = \zeta + \frac{N}{\Psi}, \tag{A 1}$$

where

$$\Psi = \left[1 + \left(\frac{\partial\zeta}{\partial S_1}\right)^2 + \left(\frac{\partial\zeta}{\partial S_2}\right)^2\right]^{1/2}. \tag{A 2}$$

The definitions of the curvilinear unit vectors for the bottom surface, $(\hat{\boldsymbol{s}}_1, \hat{\boldsymbol{s}}_2, \hat{\boldsymbol{n}})$, can be similarly obtained from the curvilinear coordinate system, (s_1, s_2, n), defined by

$$x = s_1 + \frac{n\partial\mathrm{d}/\partial s_1}{\psi}, \quad y = s_2 + \frac{n\partial\mathrm{d}/\partial s_2}{\psi}, \quad z = -\mathrm{d} + \frac{n}{\psi}, \tag{A 3}$$

where

$$\psi = \left[1 + \left(\frac{\partial\mathrm{d}}{\partial s_1}\right)^2 + \left(\frac{\partial\mathrm{d}}{\partial s_2}\right)^2\right]^{1/2}. \tag{A 4}$$

From the scaling in §2, one can easily verify that with errors of $O\left(\epsilon^6\right)$ that both sets of curvilinear unit vectors are equal to the Cartesian unit vectors $(\hat{\boldsymbol{i}}, \hat{\boldsymbol{j}}, \hat{\boldsymbol{k}})$.

Appendix B. Fourier integration

We will briefly show how to calculate indefinite integrals using Fourier methods. Let us follow Gottlieb *et al.* (1984) and represent the truncated Fourier series of the function (possibly complex) $f(x), x \in [0, 2\pi]$ as

$$f(x) = \sum_{k=-N}^{N} \frac{\hat{f}(k)}{c_k} \mathrm{e}^{\mathrm{i}kx}; \quad c_k = 2, \ k = \pm N; \quad c_k = 1, \ k \neq N. \tag{B 1}$$

This can be rewritten as

$$f(x) = \sum_{k=0}^{N-1} \hat{f}(k)\, \mathrm{e}^{\mathrm{i}kx} + \sum_{k=N}^{2N-1} \hat{f}(k)\, \mathrm{e}^{\mathrm{i}(k-2N)x} + \mathrm{i}\hat{f}(N) \sin(Nx). \tag{B 2}$$

Thus, the integral can be written

$$I(x) = \int^x f(y)\ \mathrm{d}y = \hat{f}(0)\, x - \mathrm{i}\left\{\sum_{k=1}^{N-1} \frac{\hat{f}(k)}{k} \mathrm{e}^{\mathrm{i}kx} + \sum_{k=N}^{2N-1} \frac{\hat{f}(k)}{k-2N} \mathrm{e}^{\mathrm{i}(k-2N)x} + \frac{\hat{f}(N)}{N} \cos(Nx)\right\} + g, \tag{B 3}$$

where g is a constant of integration. Now if we choose to evaluate at the Fourier grid points

$$x_j = \frac{j\pi}{N}, \quad j = 0, \ldots 2N-1, \tag{B 4}$$

https://doi.org/10.1017/S0022112097005442 Published online by Cambridge University Press

and require that the average of I is zero then we can write

$$I\left(x_j\right) = -\mathrm{i}\left\{\sum_{k=1}^{N-1}\frac{\hat{f}\,(k)}{k}\mathrm{e}^{\mathrm{i}kx_j}+\sum_{k=N}^{2N-1}\frac{\hat{f}\,(k)}{(k-2N)}\mathrm{e}^{\mathrm{i}kx_j}+(-1)^j\frac{\hat{f}\,(N)}{N}\right\}+\left[x_j-\pi\right]\hat{f}\,(0)\,. \quad \text{(B 5)}$$

The sums in the curly brackets can be found using an FFT. Clearly, if f is real, we can simplify the above expression to eliminate redundant calculations.

Appendix C. Initial profiles

For convenience, we will give the forms of the initial profiles which solve the inviscid flat-bottomed KP equation. The solutions are taken from Segur & Finkel (1985) and put into our notation.

The genus 1 (cnoidal wave) solution can be written (at $x = 0$)

$$h = \frac{4}{3}\frac{d^2\delta_x^2}{\alpha}\frac{\partial^2}{\partial r^2}\ln\theta\,(\phi;b)\,, \quad b<0, \quad \text{(C 1)}$$

where

$$\theta\,(\phi;b) = \left(\frac{2\pi}{-b}\right)^{1/2}\sum_{m=-\infty}^{\infty}\exp\left[\frac{2}{b}\left(\frac{\phi}{2}-m\pi\right)^2\right], \quad \phi = \mu r + \nu\frac{\delta_x^2}{\delta_y}y. \quad \text{(C 2)}$$

The genus 2 solution can be written (at $x = 0$)

$$h = \frac{4}{3}\frac{d^2\delta_x^2}{\alpha}\frac{\partial^2}{\partial r^2}\ln\theta\,(\phi_1,\phi_2;b,\lambda,d)\,, \quad \text{(C 3)}$$

where

$$\theta(\phi_1,\phi_2;b,\lambda,d) = \sum_{m_2=-\infty}^{\infty}\sum_{m_1=-\infty}^{\infty}\exp\left[\frac{1}{2}dm_2^2\right]\exp\left[\frac{1}{2}b\,(m_1+\lambda m_2)^2\right]\cos\left(m_1\phi_1+m_2\phi_2\right), \quad \text{(C 4)}$$

$$\phi_1 = \mu_1 r + \nu_1\frac{\delta_x^2}{\delta_y}y, \qquad \phi_2 = \mu_2 r + \nu_2\frac{\delta_x^2}{\delta_y}y, \quad \text{(C 5)}$$

$$\lambda \neq 0, \quad b<0, \quad \lambda^2 \leqslant \tfrac{1}{2}, \quad d \leqslant b\left(1-\lambda^2\right). \quad \text{(C 6)}$$

REFERENCES

Akylas T. R. 1994 Three-dimensional water-wave phenomena. *Ann. Rev. Fluid Mech.* **26**, 191–210.

Aris, R. 1989 *Vectors, Tensors, and the Basic Equations of Fluid Mechanics*. Dover.

Ascher, U., Christiansen, J. & Russell, R. D. 1981 Collocation software for boundary-value ODEs. *ACM Trans. Math Software* **7**, 209–222.

Ascher, U. M., Mattheij, R. M. M. & Russell, R. D. 1988 *Numerical Solution of Boundary Value Problems for Ordinary Differential Equations*. Prentice-Hall.

Bader, G. & Ascher, U. 1987 A new basis implementation for a mixed order boundary value ODE solver. *SIAM J. Sci. Statist. Comput.* **8**, 483–500.

Boyd, J. P. 1990 New directions in solitons and nonlinear periodic waves: polycnoidal waves, imbricated solitons, weakly nonlocal solitary waves, and numerical boundary value algorithms. *Adv. Appl. Mech.* **27**, 1–82.

https://doi.org/10.1017/S0022112097005442 Published online by Cambridge University Press

Cooley, J. W., Lewis, P. A. W. & Welch, P. D. 1970 The fast Fourier transform algorithm: programming considerations in the calculation of sine, cosine and Laplace transforms. *J. Sound Vib.* **12**, 315–337.

Gottlieb, D., Hussaini, M. Y. & Orszag, S. A. 1984 in *Spectral Methods for Partial Differential Equations* (ed. R. G. Voight *et al.*). SIAM.

Grimshaw, R. & Melville W. K. 1989 On the derivation of the modified Kadomtsev-Petviashvili equation. *Stud. Appl. Maths* **80**, 183–202.

Hammack, J., McCallister, D., Scheffner, N. & Segur, H. 1995 Two-dimensional periodic waves in shallow water. Part 2. Asymmetric waves. *J. Fluid Mech.* **285**, 95–122.

Hammack, J., Scheffner, N. & Segur, H. 1989 Two-dimensional periodic waves in shallow water. *J. Fluid Mech.* **209**, 567–589.

Hammack, J., Scheffner, N. & Segur, H. 1991 A note on the generation and narrowness of periodic rip currents. *J. Geophys. Res.* **96**, 4909–4914.

Jacobs, S. J. 1990 On wave-current interaction in a turbulent boundary layer. *Geophys. Astrophys. Fluid Dyn.* **50**, 203–227.

Jacobs, S. J. 1997 Gravity waves in a turbulent flow over a gradually sloping bottom. *J. Fluid Mech.* (to be submitted).

Johnson, R. S. 1983 The Korteweg-deVries equation and related problems in water wave theory. In *Nonlinear Waves*, (ed. L. Debnath), pp. 25–43. Cambridge University Press.

Katsis, C. & Akylas, T. R. 1987 On the excitation of long nonlinear waves by a moving pressure distribution. Part 2. Three-dimensional effects. *J. Fluid Mech.* **177**, 49–65.

Lewellen, W. S. 1977 Use of invariant modeling. In *Handbook of Turbulence*, **1** (ed. W. Frost & T. H. Moulden). Plenum Press.

Lighthill, M. J. 1978 *Waves in Fluids.* Cambridge University Press.

Longuet-Higgins, M. S. & Stewart, R. W. 1964 Radiation stresses in water waves; a physical discussion, with applications. *Deep Sea Res.* **11**, 529–562.

Mathew, J. & Akylas, T. R. 1990 On three-dimensional long water waves in a channel with sloping sidewalls. *J. Fluid Mech.* **215**, 289–307.

Mei, C. C. 1989 *The Applied Dynamics of Ocean Surface Waves.* World Scientific.

Miles, J. W. 1983 Wave evolution over a gradual slope with turbulent friction. *J. Fluid Mech.* **133**, 207–216.

Segur, H., & Finkel, A. 1985 An analytical model of periodic waves in shallow water. *Stud. Appl. Maths* **73**, 183–220.

Shuto, N. 1976 Transformations of nonlinear long waves. *ASCE Proc. 15th Coastal Engng Conf.*, pp. 423–440.

Stuart, J. T. 1966 Double boundary layers in oscillatory viscous flow. *J. Fluid Mech.* **24**, 673–687.

Van Dyke, M. 1975 *Perturbation Methods in Fluid Mechanics*, Annotated Edition. The Parabolic Press.

https://doi.org/10.1017/S0022112097005442 Published online by Cambridge University Press